Submitted to
Nuclear Physics B.

CERN/EP/PHYS 76-4
11 February 1976

PRODUCTION OF ρ^0 AND f IN $\pi^- p$ INTERACTIONS AT 16 GeV/c AND SEPARATION INTO FRAGMENTATION AND CENTRAL COMPONENTS

Aachen-Berlin-Bonn-CERN-Cracow-Heidelberg-Warsaw Collaboration

J. BARTKE(*), H. KIRK and P. SIXEL
III Physik. Inst. der Techn. Hochschule, Aachen.

H. NOWAK and M. WALTER
Inst. für Hochenergiephysik der Akad. der Wissensch.
der DDR, Berlin, Zeuthen.

K. BÖCKMANN, J. LOWSKY, R. ROEDEL and G. ZOBERNIG
Physik. Inst. der Universität, Bonn.

V.T. COCCONI, M.J. COUNIHAN, G. KELLNER, P.K. MALHOTRA(**), D.R.O. MORRISON and H. SAARIKKO(***)
CERN, European Organisation for Nuclear Research, Geneva.

E. LEITNER and J. STIEWE
Inst. für Hochenergiephysik der Univ. Heidelberg.

T. COGHEN and A. GUŁA
Inst. of Nucl. Res. and Acad. of Mining and Metallurgy,
Dept. of Phys. Cracow.

H. ABRAMOWICZ and A. ZIEMINSKI
Univ. of Warsaw and Inst. for Nuclear Research, Warsaw.

(*) Visiting Scientist from the Institute of Nuclear Physics, Cracow.

(**) Visiting Scientist from the Tata Institute of Fundamental Research, Bombay.

(***) Visiting Scientist from the Institute of Nuclear Physics, University of Helsinki.

PKM/mk

CERN/EP/PHYS 76-4

ABSTRACT

The production of $\rho^{o}(770)$ and f(1270) is studied in $\pi^{-}p$ interactions at 16 GeV/c. By comparison with inclusive K^{*o} production in the reaction $K^{-}p \to K^{*o}$ + anything, and with inclusive ρ^{o} production in the reaction $pp \to \rho^{o}$ + anything, it is found that the data can be interpreted in terms of two production processes, one central production of resonances and the other fragmentation of the beam particle. For the $\pi^{-}p$ reaction, the inclusive ρ^{o} beam fragmentation cross section is 3.1 ± 0.3 mb while that for central production is 1.6 ± 0.5 mb. The ρ^{o} central production cross section is consistent with increasing with energy as $\ell n(s)$ behaviour. The ratio of ρ^{o} to π^{-} inclusive cross sections (excluding the leading π^{-}) is $\sim$ 0.2, independent of energy. The ρ^{o} to π^{-} ratio increases as a function of p_{T} to a constant value of $\sim$ 1/2 above 1 GeV/c. The ρ (charged and neutral) and f decays account for (25 ± 4)% and (1.4 ± 0.3)%, respectively, of all pions produced.

1. INTRODUCTION

There has recently been a spurt of interest in the study of inclusive resonance production [1]. Two reasons may be cited for this. The first is the realisation that a major fraction of the pions result from the decay of resonances and therefore a study of resonances should throw light on the interaction mechanism. There are increasing indications that the observed short range correlations may in fact be due to the resonance production. The second is related to the fact that leptons are among the decay products of the meson resonances and therefore these might account for at least a part of the unexpectedly large direct production of leptons observed in nucleon-nucleon collisions at Fermilab and the ISR at CERN [2].

Inclusive ρ^o (770) production has been studied in pp interactions at 12, 24, 69 and 205 GeV/c [3]. Inclusive and semi-inclusive ρ^o, and in some cases f(1270), production has been investigated in π^+p interactions at 6 and 22 GeV/c [4] and by our collaboration at 8, 16 and 23 GeV/c [5]. In π^-p interactions some results on ρ^o production have been reported at 11.2 [6], 15 [7], 147 [8] and 205 GeV/c [9]. In this paper we present results on inclusive, semi-inclusive and exclusive ρ^o and f production in π^-p interactions at 16 GeV/c.

This investigation is based on a total of 86 142 inelastic events (4.1 events/μb) yielding a total of approximately 19 300 ρ^o and 2000 f mesons. Wherever possible, a comparison has been made with our collaboration's earlier results on π^+p interactions at 16 GeV/c [5] and with π^-p interactions at Fermilab energies.

The work described here consists of two parts. The first, in sects 2-7, deals with data on inclusive and semi-inclusive ρ^o and f production (sects 3 and 4), with ρ^o production in exclusive channels (sect. 5) and with the s-dependence and p_T-dependence of inclusive ρ^o production. The second part, in sects 8 and 9, deals with the inclusive ρ^o distribution in longitudinal momentum and rapidity, and with the

problem of separating "central" ρ^o production from ρ^o's which originate from the fragmentation of the incident pion. Sect. 10 summarises our conclusions.

3. INCLUSIVE AND SEMI-INCLUSIVE DIPION MASS SPECTRA

Fig. 1 shows the dipion ($\pi^+\pi^-$) mass spectrum $d\sigma/dM$ for the inclusive reaction

$$\pi^- p \to \pi^- \pi^+ + \text{anything}. \qquad (1)$$

The errors are not shown as they are smaller than the size of the points drawn. The overall shape of the spectrum is very similar to that seen in $\pi^+ p$ interactions at 16 GeV/c [5]. The ρ^o signal is clearly visible and there is indication of a structure in the mass region of the f. There are nearly 19 300 events above the background in the ρ^o peak.

Fig. 2 shows the $\pi^+\pi^-$ mass spectra for different charged multiplicities in the final state. The ρ^o and f signals are the strongest for the 2-prong events and both decrease as the multiplicity increases. These plots also indicate that apart from the resonance signals the spectrum is nearly exponential, with the exponent increasing with the multiplicity. The inclusive spectrum shown in fig. 2(f) is described approximately by exp (-2.3 M). Fig. 3 shows the inclusive mass spectrum multiplied by a factor exp (2.3 M) to compensate for the sharply falling background. This brings out the resonance signals rather clearly. All these features are basically similar to those obtained in our study of $\pi^+ p$ interactions at 16 GeV/c [5].

3. RESONANCE FITTING

The method employed to fit the mass spectrum to deduce the resonance cross section is essentially the same as described earlier in ref. [5]. The reader is therefore referred to it for details.

To determine the differential distribution of ρ^o (or f) with respect to any variable, e.g. p_T^2, the data are first divided into suitable bins in that variable and the resonance signals are then obtained by fitting the corresponding dipion mass spectra. The fits were generally quite good, as may be seen from $\chi^2/NDF = 148/138 = 1.1$ obtained for a set of fits for the ρ^o to the mass spectra and $\chi^2/NDF = 45/40 = 1.1$ for the f. The overall excellent consistency of the fits obtained is demonstrated by table 1, which gives the values of the cross section for ρ^o production (the errors given here are statistical only) obtained by summing up the partial cross sections using selections in charged multiplicity (semi-inclusive), the transverse momentum squared (p_T^2), the Feynman variable (x) and the c.m. rapidity (y^*).

4. INCLUSIVE AND SEMI-INCLUSIVE CROSS SECTIONS

Table 2 summarises the results of the fits to the $\pi^+\pi^-$ mass spectra in π^-p interactions at 16 GeV/c. The value given in the table 2 for the inclusive $\sigma(\rho^o)$ is the average of the values (see table 1) estimated using five different methods. Clearly, there is appreciable production of ρ^o at this energy - approximately one ρ^o is produced in every 4 or 5 inelastic interactions. Compared to ρ^o, the production of f is down by a factor of about 5. For comparison, we have included also the results on π^+p interactions at the same beam momentum [5]. The individual cross sections, as well as the average numbers (per inelastic interaction) of ρ^o and f for π^-p interactions are equal to those for π^+p interactions.

Errors given in table 2 (and throughout this paper, unless otherwise mentioned) include both the statistical and systematic uncertainties arising from the fitting procedure, exclusion of events with visible strange particle decays (we have assumed these events to have characteristics similar to the rest of the events) and the values of inelastic cross section and topological cross sections used for normalization. Unless mentioned otherwise, the numbers relating to f production are obtained from the observed $f \to \pi^+\pi^-$ mode by multipling the latter by a factor 1.81 ± 0.11 to take into account the unseen decay modes.

A quantity of considerable interest is the ratio of the average number of ρ^o (and f) to the average number of pions. However, for a meaningful comparison between π^-p and π^+p interactions at 16 GeV/c, particularly at these low energies, it is important to take into account the strong leading particle effect and the influence of the charge conservation. For this reason, we define a quantity $<\pi_c>$ as a measure of the "created" pions(*). In the case of π^+p and pp interactions, it is natural to take $<\pi_c> = <\pi^->$, since the leading particle effect and the charge conservation are expected to have minimum influence on $<\pi^->$. However, for π^-p interactions we take $<\pi_c> = (<\pi^-> -1)$, i.e. $<\pi^->$ minus the leading π^-, rather than $<\pi^+>$, since there is significant contribution to $<\pi^+>$ from events involving a neutron in the final state. The table 2 shows that the ratio $R \equiv <\rho^o>/<\pi_c> = 0.20 \pm 0.02$ for π^-p interactions and 0.19 ± 0.02 for π^+p interactions, indicating that R is independent of the charge of the beam pion. We therefore conclude that if the effects of the charge conservation and the leading particle behaviour are taken into account, the ratio of $<\rho^o>$ to the average number of "created" pions in π^-p collisions is equal to that in π^+p collisions. Similar observations hold also for the f meson.

The semi-inclusive (i.e. broken down according to n, the charged multiplicity) cross sections and the average number, per event, of ρ^o and $f \to \pi^+\pi^-$ are presented in tables 3 and 4. Figs 4(a) and (b) show $\sigma(\rho^o)$ and $\sigma(f \to \pi^+\pi^-)$ as functions of charged multiplicity for both π^-p and π^+p interactions at 16 GeV/c. The bulk of the production (in terms of cross section) takes place in 4 and 6-prong events for ρ^o and 2, 4 and 6-prong events for the f. The semi-inclusive distributions for $\sigma(\rho^o)$ are similar for π^-p and π^+p interactions. Fig. 4(b) indicates that this is not true for $f \to \pi^+\pi^-$ (the detected mode). In order to ascertain whether this is merely due to the fact that we detect the mode $f \to \pi^+\pi^-$ (branching ratio = 0.55 ± 0.04) only, or there is a more important reason for it, we have calculated the semi-inclusive cross sections for f (all decay

---

(*) Average number of created charged pions = $2<\pi_c>$

modes) from the measured semi-inclusive cross sections for the partial mode $f \to \pi^+\pi^-$, using the known branching ratios (as a function of multiplicity) for the f-decay. This is shown in fig. 4(c). It is clear that except for the 4-prong events, the semi-inclusive cross sections for f production in π^-p and π^+p interactions are comparable. The difference between 4-prong cross section for f production in π^+p and π^-p collisions is probably due to the relatively large cross section ($\sim$ 130 μb) for the quasi two-body reaction $\pi^+p \to f\Delta^{++}$.

Fig. 5 shows the ratio $\langle\rho^o\rangle/\langle\pi^+\rangle$ (i.e. ρ^o relative to the pions of charge opposite to the beam) as a function of the charged multiplicity n. This ratio seems to be slightly decreasing with increasing multiplicity for $n \geq 4$. This may be compared with the dependence of $R(\pi^+p) = \langle\rho^o\rangle/\langle\pi^-\rangle$ on multiplicity in π^+p collisions at 16 GeV/c, which is also shown in the same figure. The two ratios behave somewhat differently. As pointed out earlier in this section, this difference is largely due to charge conservation. For this reason, the ratio $R(\pi^-p) = \langle\rho^o\rangle/(\langle\pi^-\rangle - 1)$ for π^-p interactions is also shown in fig. 5. This seems to be in good agreement with $R(\pi^+p) = \langle\rho^o\rangle/\langle\pi^-\rangle$ for π^+p interactions. It may be noted that the decrease in the ratio R with increasing multiplicity is even more pronounced than the decrease of $\langle\pi^o\rangle/\langle\pi^-\rangle$ observed at comparable energies [10]. This can be qualitatively understood as due to the decrease of phase space for ρ^o with increasing multiplicity and also to the fact that the relative contribution of ρ^o arising from the fragmentation (see sects 8 and 9) of the beam pion decreases as the multiplicity increases.

The table 4 also includes the ratio $\langle f \to \pi^+\pi^-\rangle/\langle\rho^o\rangle$, i.e. the average number of $f \to \pi^+\pi^-$ to the average number of ρ^o, as a function of the charged multiplicity. It may be noted that this ratio for the 2-prongs is 0.38 ± 0.13, which is rather large compared to the inclusive value of 0.11 ± 0.02. This is due to the fact that in quasi two-body channels f and ρ^o cross sections are comparable, e.g. our fits indicate that $\sigma(\pi^-p \to \rho^o n) = 55 \pm 15$ μb (*) and $\sigma(\pi^-p \to fn) = 48 \pm 20$ μb.

(*) This value is consistent with the value of 45 ± 12 μb deduced earlier [11].

5. EXCLUSIVE CHANNELS

Table 5 presents the results on cross section and average number of ρ^o's in a variety of exclusive channels. It is interesting to study the energy dependence and the x distribution of $\sigma(\rho^o)$ to learn more about the reaction mechanisms responsible for some of the exclusive channels. For example, as we shall see in sect. 8, the reaction $\pi^- p \to \rho^o n$ is so peripheral that almost all the ρ^o's fall in the extreme forward bin of $0.95 < x < 1.0$.

6. ENERGY DEPENDENCE OF INCLUSIVE ρ^o PRODUCTION

The energy dependence of average charged multiplicity has been studied by many authors [see e.g. refs 10, 12 and 13]. Since a substantial fraction of pions result from ρ-decay, it would be useful to ascertain the energy dependence of the average multiplicity of ρ.

Figs 6 and 7(a) show the dependence of the inclusive ρ^o cross section $\sigma(\rho^o)$ and the average ρ^o multiplicity $\langle\rho^o\rangle$ on s, the square of the c.m. energy, for $\pi^- p$ [7-9], $\pi^+ p$ [4-5] and pp [3] interactions. As the data are meagre, we have used the simple variable s rather than for example the available energy, and have carried out fits of the form

$$\sigma(\rho^o) = a + b\ \ell n(s) \tag{2}$$

$$\langle\rho^o\rangle = c + d\ \ell n(s) \tag{3}$$

to the combined $\pi^{\pm} p$ data for $s \geq 15.9$ GeV^2 ($p_{lab} \geq 8$ GeV/c). The fits, shown as solid lines in figs 6 and 7(a), are quite good (χ^2/NDF = 4.5/6, and 5.5/6, respectively) and the values of the parameters (with s in GeV^2) are found to be

$$\left.\begin{aligned} a(\rho^o) &= -2.0 \pm 0.2 \text{ mb} \\ b(\rho^o) &= 1.97 \pm 0.06 \text{ mb} \end{aligned}\right\} \tag{4}$$

$$\left.\begin{aligned} c(\rho^o) &= -0.08 \pm 0.01 \\ d(\rho^o) &= 0.09 \pm 0.01. \end{aligned}\right\} \tag{5}$$

The values of $c(\rho^o)$ and $d(\rho^o)$ may be compared to the corresponding values [13] for π^- production in π^+p interactions,

$$\left.\begin{aligned} c(\pi^-) &= -1.11 \pm 0.10 \\ d(\pi^-) &= 0.67 \pm 0.04. \end{aligned}\right\} \qquad (6)$$

Thus, the coefficient of the $\ell n(s)$ term is considerably greater for $<\pi^->$ than for $<\rho^o>$. The s-dependences for $\sigma(\rho^o)$ and $<\rho^o>$ in pp interactions seem to be similar to those in pp interactions as can be seen from the dotted lines which represent fits to the pp data with slopes constrained to the corresponding $\pi^\pm p$ values. The values of a and c for pp data are

$$a(\rho^o) = -4.4 \pm 0.4 \text{ mb} \qquad (7)$$

$$c(\rho^o) = -0.23 \pm 0.03. \qquad (8)$$

The implications of the different values for the parameter c in $\pi^\pm p$ and pp interactions will be discussed in sect. 9.

Fig. 7(b) shows the s-dependence of the ratio $R = <\rho^o>/<\pi_c>$ (see sect. 4) for π^-p, π^+p and pp interactions. Once again, we see that this ratio seems to have similar values for π^-p and π^+p interactions. For $p_{lab} \lesssim 205$ GeV/c, R is far smaller for pp interactions than for $\pi^\pm p$ interactions. In each case, the ratio seems to have very slow, if any, s-dependence. The solid curve in fig. 7(b) is the prediction based on the solid line in fig. 7(a), i.e. with the coefficients of eqs (5), and eqs (6). Likewise the dashed line in fig. 7(b) is the prediction based on the dashed line in fig. 7(a) and a fit to the experimental data on the energy dependence of $<\pi^->$ in pp collisions. It is interesting to note that the curves exhibit a tendency to approach asymptotic limits from above for $\pi^\pm$ and from below for pp.

7. TRANSVERSE MOMENTUM DISTRIBUTIONS

Fig. 8 shows the distribution in p_T^2, the square of the transverse momentum, of the ρ^o, which was obtained by following the procedure outlined in sect. 3. The fits are consistently good as can be judged from the

overall $\chi^2/NDF = 88/94 = 0.94$. The integral cross section for ρ^o is found to be 4.73 mb, in agreement with the values for $\sigma(\rho^o)$ given in table 2.

A salient feature of the distribution is that for $0.2 < p_T^2 < 2.0$ $(GeV/c)^2$, the ρ^o differential cross section is well represented by the exponential function (dashed line in fig. 8)

$$\frac{d\sigma(\rho^o)}{dp_T^2} = A\, e^{-B\, p_T^2} \tag{9}$$

with

$$\left.\begin{aligned} A &= 10.7 \pm 1.2 \quad \text{mb } (GeV/c)^{-2} \\ B &= 2.94 \pm 0.15 \quad\; (GeV/c)^{-2}. \end{aligned}\right\} \tag{10}$$

Another characteristic feature of the distribution is that in the region of $p_T^2 < 0.2$ $(GeV/c)^2$, the dependence on p_T^2 becomes steeper towards $p_T^2 = 0$. If the distribution for $p_T^2 < 0.2$ $(GeV/c)^2$ is also represented by the exponential form (9), then we obtain $A' = 21.8 \pm 1.2$ mb $(GeV/c)^{-2}$ and $B' = 5.5 \pm 0.5$ $(GeV/c)^{-2}$.

We have also fitted the ρ^o distribution with an expression of the type

$$\frac{d\sigma(\rho^o)}{dp_T^2} = A_1\, e^{-B_1\, p_T^2} + A_2\, e^{-B_2 p_T^2}. \tag{11}$$

The fit obtained is good ($\chi^2/NDF = 10.4/9$) and the values of the parameters are

$$\left.\begin{aligned} A_1 &= 13.9 \pm 2.0 \text{ mb } (GeV/c)^{-2} \\ B_1 &= \;\; 9.6 \pm 1.5 \;\; (GeV/c)^{-2} \\ A_2 &= \;\; 9.2 \pm 1.5 \text{ mb } (GeV/c)^{-2} \\ B_2 &= \;\; 2.8 \pm 0.2 \;\; (GeV/c)^{-2}. \end{aligned}\right\} \tag{12}$$

Thus the steeper region has a slope ~ 9.6 compared to ~ 2.8 for the flatter region.

For comparison, fig. 8 also shows the p_T^2 distribution for π^+ and a few representative points for π^-. The low p_T^2 peak is much more pronounced for $\pi^\pm$ than for the ρ^o. What is particularly interesting is the fact that above about 1 $(GeV/c)^2$ the p_T^2 distributions for π^+ and π^- are also nearly exponential and the exponent has a value very similar to that of the ρ^o distribution. Fig. 9 shows the ratio of the cross section of ρ^o to that of π^+ as a function of p_T^2. This ratio increases rather fast at low p_T^2 and is consistent with a constant value $\sim 0.54 \pm 0.06$ for $0.8 < p_T^2 < 2.5$ $(GeV/c)^2$. This may be contrasted with the ratio $\sigma(\rho^o)/\sigma(\pi^-)$ for 16 GeV/c π^+p [5], which was found to level off approximately at a value ~ 1. This difference between the ratio of $\sigma(\rho^o)/\sigma(\pi^-)$ for π^+p interactions and $\sigma(\rho^o)/\sigma(\pi^+)$ for π^-p interactions implies that the influence of the proton charge is felt even in the region of $p_T^2 > 1(GeV/c)^2$. This effect is similar to the ISR observation that $(\pi^+/\pi^-) > 1$ at large p_T, in pp interactions.

Table 6 gives $\langle p_T^2 \rangle$ and $\langle p_T \rangle$ for ρ^o, π^+ and π^- in π^-p and π^+p interactions at 16 GeV/c. It is interesting to note that: (i)$\langle p_T^2 \rangle$ for ρ^o has nearly the same value in π^-p and π^+p interactions and (ii) in both cases it is considerably greater than $\langle p_T^2 \rangle$ for $\pi^\pm$; this is in accord with the well known observation that the average $\langle p_T^2 \rangle$ increases with the mass of the particle.

8. LONGITUDINAL MOMENTUM AND RAPIDITY DISTRIBUTIONS FOR ρ^o

The distribution of ρ^o's in terms of the Feynman variable $x = p^*_{//}/p^*_{max}$ and of p_T has been studied in some detail. Here, p^*_{max} is the maximum possible momentum for the ρ^o in the c.m. system and is taken to be a function of the dipion mass. Figs 10 and 11 show the non-invariant and invariant distributions, respectively. At low transverse momentum ($p_T < 0.2$ GeV/c), the distributions show striking forward peaks characteristic of the fragmentation processes. As p_T increases, this effect becomes less pronounced and proportionately more ρ^o's are produced in the central region. Figs 10(b) and 11(b) show the x distribution, integrated

over all p_T. The maximum of the invariant cross section lies at $x \sim 1$ and there is no distinct peak at $x = 0$ for the central ρ^o production. The ratio of ρ^o's produced forward to those produced backwards in the c.m. system is 3.6 ± 0.3. These facts indicate that: (i) the beam fragmentation component is larger than the central component and (ii) the x-distributions of the two components overlap considerably. There is no evidence for any significant production of ρ^o in the target framentation region.

Fig. 12 shows a comparison of invariant x distributions for ρ^o cross section in $\pi^- p$ and $\pi^+ p$ interactions at 16 GeV/c. There is no significant difference between the two reactions. However, the invariant cross section seems to be systematically slightly greater for $\pi^- p$ interactions than for $\pi^+ p$ interactions, particularly in the forward direction. This difference could arise from channels such as $\pi^- p \to \rho^o n$ and $\pi^- p \to \rho^o n\pi^o$. For example, the x distribution (fig. 12) for the channel $\pi^- p \to \rho^o n$ is sharply peaked forward; in fact, the entire 55 μb cross section for this channel falls in the forward bin $0.95 < x < 1.0$. Furthermore, since the ρ^o's in such reactions have relatively higher energies, this tends to increase the invariant cross section in the forward direction.

In fig. 13 the x distribution for inclusive ρ^o production is compared with the same for π^+ and π^- in $\pi^- p$ interactions. These distributions are quite different. Also shown for comparison is the distribution for the reaction $K^- p \to K^{*o}(890)$ + anything at 16 GeV/c [14]. This reaction is of great interest since at these low energies K^{*o} is expected to be produced almost exclusively through the fragmentation of the K^-. In this respect it is encouraging to note that the distribution of K^{*o} is similar, both in shape and magnitude, to that of ρ^o in the region of $x \gtrsim 0.5$. At lower values of x the distributions differ considerably because of the central production of ρ^o. The ρ^o and K^{*o} distributions will be used in sect. 9 to deduce the x distribution of the central production of the ρ^o.

Fig. 14 shows the x distributions of the ρ^o invariant cross section, integrated over the transverse momentum, for different charged multiplicities. For low multiplicities, i.e. 2 and 4-prongs, the distributions show pronounced forward peaks characteristic of the fragmentation (beam) processes. For 6- and 8-prongs, the maximum is shifted towards smaller values of x, but there is still some excess in the forward direction over the backward direction.

The differential distribution of the ρ^o rapidity in the beam frame, namely $y_b(\rho^o) = y_{beam} - y(\rho^o)$ is presented in fig. 15. For comparison, available data from π^-p interactions at 147 GeV/c [8] and 205 GeV/c [9] are also shown. These data indicate that in the beam fragmentation region there is no significant variation of $d\sigma/dy_b$ with p_{lab}.

Fig. 16 presents ρ^o density $(1/\sigma_{inel})(d\sigma(\rho^o)/dy^*)$ as a function of the c.m. rapidity y^* in π^-p interactions at 16 GeV/c. For comparison, the results for π^+p interactions [5] at the same energy are also shown. Once again, the two distributions look very similar. Also shown in the same figure is the ρ^o density distribution in pp interactions at 24 GeV/c obtained by Blobel et al. [3]. The pp data at 24 GeV/c are chosen because they correspond to nearly the same "available energy" ($Q = \sqrt{s} - 2m_p$) as the π^-p interactions at 16 GeV/c ($Q = \sqrt{s} - M_p - m$). It is interesting to note that: (i) the ρ^o distribution for pp interactions exhibits the characteristics of dominantly central production and (ii) the pp distribution in the region $y^* \lesssim (-0.3)$ approximately overlaps that of the $\pi^\pm p$ distribution. The point (ii) leads us to the important conclusion that the y^* distribution and also the overall magnitude of the central component (including a small contribution from the target proton fragmentation) of the ρ^o production in $\pi^\pm p$ collisions are very similar to those of the ρ^o production in pp collisions.

9. ρ^o COMPONENTS - BEAM FRAGMENTATION AND CENTRAL

As mentioned in the preceeding section, the dominant sources of the ρ^o production in $\pi^- p$ interactions, namely the central and the beam fragmentation, overlap considerably in x and y^*. We are therefore reluctant to evaluate their relative magnitudes by making arbitrary cuts in x or in y^* as has been suggested previously [7]. Instead, two other approaches have been followed to estimate the magnitudes of the central and the beam fragmentation components for the ρ^o production in $\pi^- p$ interactions at 16 GeV/c.

In the first approach we assume that the distribution of the invariant cross section pertaining to the beam fragmentation (F) component of ρ^o is similar to that of the distribution of the invariant cross section of $K^{*o}(890)$ in the reaction $K^- p \to K^{*o}$ + anything at 16 GeV/c. This assumption is plausible since: (i) the K^{*o} production in the latter reaction should originate dominantly from beam fragmentation (multiple strange particle production is rare) at these relatively low energies and (ii) the kinematic factors do not differ greatly since the masses of ρ^o and K^{*o} are comparable. Fig. 13 shows that in the region of $x \gtrsim 0.4$ the distribution for $K^- p \to K^{*o} X^o$ coincides with that of $\pi^- p \to \rho^o X^o$. In view of this observation we feel it reasonable to assume that the distribution for the fragmentation component of the ρ^o is not only similar but also equal in magnitude to that of the overall K^{*o} distribution. If this assumption is true, then the difference of the two distributions should yield the distribution of the central component of the ρ^o, which should therefore be approximately symmetric about x = 0. The actual difference in the two experimental distributions is shown in fig. 17. It is encouraging to note that this distribution has indeed the characteristics of the central component. It therefore follows that the cross section for the ρ^o resulting from the fragmentation of the beam π^- should be equal to the cross section for K^{*o} production by fragmentation of the K^-, namely

$$\sigma_F(\pi^- p \to \rho^o X^o) = \sigma(K^- p \to K^{*o} X^o) = 3.2 \pm 0.4 \text{ mb}.$$

This should however be corrected for the small amount of central production

of the K^{*o}. We have estimated this correction to be 0.2 ± 0.1 mb from a study of the differential distributions for $K^- p \to K^{*+} X^-$) [14] and $\pi^+ p \to K^{*+} X^+$ [15], both at 16 GeV/c. Thus, the corrected value for the beam fragmentation component of ρ^o in 16 GeV/c $\pi^- p$ interactions, resulting from this first method, is

$$\sigma_F^{(1)} \ (\pi^- p \to \rho^o X^o) = 3.0 \pm 0.4 \text{ mb}. \qquad (13)$$

In the second approach we make the following plausible assumptions: (i) in pp interactions the entire ρ^o production takes place via the central mechanism only (we ignore a possible small contribution due to the proton fragmentation) and (ii) the central production of ρ^o (i.e. $\langle\rho^o\rangle_C$) in $\pi^- p$ interactions is equal to that in pp interactions at the same value of $\sqrt{s}$, the c.m. energy and (iii) the fragmentation component is independent of energy and the entire energy dependence of $\langle\rho^o\rangle$ arises from the central component. The difference in the intercepts of the s dependence (see sect. 6) of the $\langle\rho^o\rangle$ for $\pi^- p$ and pp interactions should then yield the $\langle\rho^o\rangle$ for the beam fragmentation component. Thus, from eqs (5) and (8)

$$\langle\rho^o\rangle_F = c_{\pi^- p} \ (\rho^o) - c_{pp} \ (\rho^o) = 0.15 \pm 0.01. \qquad (14)$$

Therefore, the cross section of the fragmentation component deduced from the second approach is

$$\sigma_F^{(2)} \ (\pi^- p \to \rho^o X^o) = \langle\rho^o\rangle_F \cdot \sigma_{inel} \ (\pi^- p) = 3.1 \pm 0.3 \text{ mb}, \qquad (15)$$

This value agrees well with the one deduced earlier (eq. 13). It is interesting to note that the two different approaches lead to similar values for the cross section for the ρ^o arising from the fragmentation of the beam π^-. The average of the values of eqs (13) and (15) is

$$\sigma_F(\rho^o) = 3.1 \pm 0.3 \text{ mb}. \qquad (16)$$

The cross section for the central component for ρ^o in the reaction $\pi^- p \to \rho^o X^o$ at 16 GeV/c is then given by

$$\sigma_C(\pi^- p \to \rho^o X^o) = (4.73 \pm 0.4) - (3.1 \pm 0.3) = 1.6 \pm 0.5 \text{ mb}. \quad (17)$$

The energy dependence of the average number of ρ^o per interaction arising from the central component, assumed to be the same for $\pi^{\pm} p$ and pp interactions, can be expressed as

$$\langle \rho^o \rangle_C = (-0.23 \pm 0.03) + (0.09 \pm 0.01)\, \ell n(s). \quad (18)$$

10. DISCUSSION AND CONCLUSIONS

From this study of ρ^o and f production in $\pi^- p$ interactions at 16 GeV/c, the following conclusions can be drawn:

(a) The inclusive ρ^o cross section is large: $\sigma(\pi^- p \to \rho^o X^o) = 4.73 \pm 0.4$ mb. The average number of ρ^o per inelastic interaction is $\langle \rho^o \rangle = 0.23 \pm 0.02$. Assuming that: (i) $(\langle \rho^+ \rangle + \langle \rho^- \rangle) = 2 \langle \rho^o \rangle$ and (ii) $\langle \pi^o \rangle = 0.5\, (\langle \pi^+ \rangle + \langle \pi^- \rangle)$, it is found that $(25 \pm 4)\%$ of all pions are products of ρ decays(*). In the same way f-decay accounts for $(1.4 \pm 0.3)\%$ of all pions. Similar values are found for $\pi^+ p$ interactions at 16 GeV/c.

The energy dependence of ρ^o production in $\pi^{\pm} p$ and pp interactions can be represented as

$$\sigma(\rho^o) = 2.0\, \ell n(s) + \text{constant}$$
$$\langle \rho^o \rangle = 0.09\, \ell n(s) + \text{constant}$$

where s is in GeV^2.

(b) The inclusive f cross section is $\sigma(\pi^- p \to f X^o) = 0.92 \pm 0.13$ mb, i.e. 20% of the ρ^o cross section.

(*) If we remove one negative pion per interaction as the leading pion, then ρ-decay accounts for $(34 \pm 6)\%$ of all pions.

(c) The leading particle effect and the charge conservation are found to influence strongly the relative yields of ρ and π. The influence of these effects can be minimized by defining a ratio $R \equiv \langle\rho^o\rangle/\langle\pi_c\rangle$, with $\langle\pi_c\rangle = \langle\pi^-\rangle$ for π^+p (and pp) interactions and $\langle\pi_c\rangle = (\langle\pi^-\rangle - 1)$ for π^-p interactions. At 16 GeV/c, $R(\pi^-p) = 0.20 \pm 0.02$ and $R(\pi^+p) = 0.19 \pm 0.02$, i.e. R is independent of the charge of the beam pion.

The ratio R exhibits extremely weak energy dependence, if any, for both $\pi^\pm p$ and pp interactions. Furthermore, $R(\pi^\pm p) > R(pp)$ at least up to 205 GeV/c. These features support the picture outlined in (f) below.

(d) Over the range $0.2 < p_T^2 < 2.0$ $(GeV/c)^2$, the p_T^2 distribution of the ρ^o is well represented by the exponential form $d\sigma(\rho^o)/dp_T^2 = 10.7\ e^{-2.9\ p_T^2}$ mb $(GeV/c)^{-2}$. For $p_T^2 < 0.2$, the distribution exhibits a fairly sharp peak towards $p_T = 0$ due to the beam fragmentation. The ratio $\sigma(\rho^o)/\sigma(\pi^+)$ increases with p_T^2 in the range 0 to about 1 $(GeV/c)^2$ where it levels off at a value of ~ 0.54. Thus, for $p_T^2 \gtrsim 1$ $(GeV/c)^2$, the ρ^o and π^+ exhibit very similar p_T^2 dependence.

(e) There is clear evidence that the ρ^o production in π^-p interactions is dominated by two components, namely beam fragmentation and central component. This is suggested by the observed strong peak at $x = 1$ in the double differential distributions in x and p_T, invariant and non-invariant, for $0 < p_T^2 < 0.2$ GeV/c and the rather large value (3.6 ± 0.3) for the forward to backward ratio in the c.m. system for the ρ^o.

Of the inclusive cross section of ρ^o in the reaction $\pi^-p \to \rho^oX^o$ at 16 GeV/c, it is estimated that $\sigma_F(\rho^o) = 3.1 \pm 0.3$ mb arises from the fragmentation of the beam π^- and $\sigma_C(\rho^o) = 1.6 \pm 0.5$ mb from the central production. These estimates have been arrived at in two independent ways. If the beam fragmentation component is assumed to be independent of energy, then the energy dependence of the central component, assumed to be same for πp and pp interactions, is

$$\langle\rho\rangle_C = -0.23 + 0.09\ \ell n(s).$$

(f) The production of ρ^o in $\pi^\pm p$ and pp interactions and that of $K^{*o}(890)$ in $K^- p$ interactions are consistent with the following picture. There are in general two components responsible for the production of these resonances, namely, the beam fragmentation (for $\pi^\pm$ and K^-) and the central component (the proton fragmentation component is relatively small). While the fragmentation component is constant (or nearly so), the central component grows slowly with s, e.g. like $\ell n(s)$. There is mainly one component responsible for ρ^o production (at least at moderate energies) in pp interactions, namely the central component. On the other hand in $\pi^\pm p$ interactions, both components are present, the central component ($\langle\rho^o\rangle_C$) being equal to that in pp interactions. From eqs (14) and (18) we find that in $\pi^\pm p$ interactions the beam fragmentation component and the central component become equal (3.1 mb) at $s \sim 65$ GeV^2, the former dominating at lower energies and the latter at higher energies. The K^{*o} production in $K^- p$ interactions is expected to follow a behaviour similar to the ρ^o production in $\pi^- p$ interactions, with the important difference that the central component would become important only at relatively higher energies (since it requires multiple strange particle production).

We are greatly indebted to the operating crews of the CERN proton synchrotron, of the 200 cm CERN hydrogen bubble chamber and the constructors of the beam. We would also like to thank the scanning, measuring and computing staffs in all our laboratories.

REFERENCES

[1] F.C. Winkelmann, Review talk at the IVth Int. Conf. on Experimental Meson Spectroscopy (1974), Report LBL-3045 (1974).
K. Böckmann, Rapporteur's talk at the Int. Conf. on High-Energy Phys., Palermo (1975).

[2] J.P. Boymond et al., Phys. Rev. Lett. 33 (1974) 112.
J.A. Appel et al., Phys. Rev. Lett. 33 (1974) 722.
F.W. Büsser et al., Phys. Lett. 53B (1974) 212.
B.G. Pope, Rapporteur's talk at the Int. Conf. on High-Energy Phys., Palermo (1975).

[3] V. Blobel et al., Phys. Lett. 48B (1974) 73.
V.V. Ammosov et al., Palermo Conf. paper (1975).
R. Singer et al., Preprint ANL-HEP-PR-75-48.

[4] H.A. Gordon et al., Phys. Rev. Lett. 34 (1975) 284.

[5] Aachen-Berlin-Bonn-CERN-Cracow-Heidelberg-Warsaw Collaboration, M. Deutschmann et al., Palermo Conf. paper (1975) and submitted to Nucl. Phys. B (1975).

[6] P. Borzatta et al., Nuovo Cimento 15A (1973) 45.

[7] J. Brau et al., Nucl. Phys. B99 (1975) 232

[8] D. Fong et al., Phys. Lett. 60B (1975) 124.

[9] F.C. Winkelmann et al., Phys. Lett. 56B (1975) 101.

[10] J. Whitmore, Physics Reports 10 (1974) 273.

[11] Aachen-Berlin-Bonn-CERN-Cracow-Heidelberg-Warsaw Collaboration, J. Bartsch et al., Nucl. Phys. B46 (1972) 46.

[12] S.N. Ganguli and P.K. Malhotra, Phys. Lett. 42B (1972) 83.
A.M. Rossi et al., Nucl. Phys. B84 (1975) 269.

[13] G.A. Akopdjanov et al., Nucl. Phys. 75B (1974) 401.

[14] Aachen-Berlin-CERN-London-Vienna-Collaboration (to be published). Private communication from H. Saarikko.

[15] Aachen-Berlin-Bonn-CERN-Cracow-Heidelberg-Warsaw Collaboration. Private communication from J. Lowsky.

TABLE CAPTIONS

Table 1 Cross section for ρ^o production, in $\pi^- p$ interactions at 16 GeV/c, obtained by summing up the partial cross sections calculated by fitting the mass spectra resulting from cuts in charged multiplicity, transverse momentum squared, Feynman variable and the c.m. rapidity. The value obtained from the fit to the inclusive dipion ($\pi^+\pi^-$) mass distribution is also included. The errors given here are statistical only.

Table 2 Cross sections, average multiplicities and particle ratios for ρ^o, f, π^- and π^+ in $\pi^- p$ and $\pi^+ p$ [5] interactions at 16 GeV/c. The numbers of f are obtained from $f \to \pi^+\pi^-$ by applying a correction factor of 1.81 ± 0.11 to take into account the unseen decay modes. The quantity $\langle\pi_c\rangle$ is equal to $\langle\pi^-\rangle$ and $(\langle\pi^-\rangle - 1)$ for $\pi^+ p$ interactions and $\pi^- p$ interactions, respectively (see text). See text also for a discussion of errors.

Table 3 $\sigma(\rho^o)$, $\langle\rho^o\rangle$ and $\langle\rho^o\rangle/\langle\pi^+\rangle$ for different charged multiplicities in $\pi^- p$ interactions at 16 GeV/c.

Table 4 $\sigma(f \to \pi^+\pi^-)$, $\langle f \to \pi^+\pi^-\rangle$, $\langle f \to \pi^+\pi^-\rangle/\langle\pi^+\rangle$ and $\langle f \to \pi^+\pi^-\rangle/\langle\rho^o\rangle$ for different charged multiplicities.

Table 5 $\sigma(\rho^o)$ and $\langle\rho^o\rangle$ for various exclusive channels. The third column gives the cross section for each exclusive channel considered.

Table 6 Average transverse momentum squared and average transverse momentum for ρ^o, π^+ and π^- in $\pi^- p$ and $\pi^+ p$ interactions at 16 GeV/c.

TABLE 1

ρ^o TOTAL CROSS SECTION DEDUCED IN DIFFERENT WAYS	
Fitting procedure	$\sigma(\rho^o)$ (mb)
Multiplicity bins	4.68 ± 0.16
p_T^2 bins	4.73 ± 0.16
x bins	4.81 ± 0.16
y^* bins	4.76 ± 0.17
Inclusive fit	4.67 ± 0.16
Average	4.73 ± 0.16

TABLE 2

ρ^0 AND f PRODUCTION IN $\pi^\pm$ INTERACTIONS AT 16 GeV/c		
Quantity	$\pi^- p$	$\pi^+ p$ [5]
$\sigma(\rho^0)$ (mb)	4.7 ± 0.4	4.8 ± 0.4
$\langle\rho^0\rangle$	0.23 ± 0.02	0.24 ± 0.02
$\langle\rho^0\rangle/\langle\pi_c\rangle$	0.20 ± 0.02	0.19 ± 0.02
$\sigma(f)$ (mb)	0.92 ± 0.13	0.99 ± 0.10
$\langle f\rangle$	0.043 ± 0.007	0.050 ± 0.005
$\langle f\rangle/\langle\pi_c\rangle$	0.037 ± 0.006	0.040 ± 0.004
$\langle\pi^-\rangle$	2.15 ± 0.01	1.25 ± 0.01
$\langle\pi^+\rangle$	1.57 ± 0.01	2.55 ± 0.01

TABLE 3

ρ^o PRODUCTION AS A FUNCTION OF MULTIPLICITY IN $\pi^- p$ INTERACTIONS AT 16 GeV/c							
Prongs	2	4	6	8	10	12	ALL
$\sigma(\rho^o)$ (mb)	0.26 ± 0.07	1.99 ± 0.22	1.60 ± 0.17	0.70 ± 0.10	0.10 ± 0.03	0.03 ± 0.03	4.68 ± 0.40
$<\rho^o>$	0.04 ± 0.01	0.22 ± 0.02	0.33 ± 0.04	0.51 ± 0.07	0.50 ± 0.15	-	0.23 ± 0.02
$<\rho^o>/<\pi^+>$	0.07 ± 0.02	0.16 ± 0.02	0.14 ± 0.01	0.15 ± 0.02	0.11 ± 0.03	-	0.15 ± 0.02

TABLE 4

$(f \to \pi^+\pi^-)$ PRODUCTION AS A FUNCTION OF MULTIPLICITY IN $\pi^- p$ INTERACTIONS AT 16 GeV/c						
Prongs	2	4	6	8	10	ALL
$\sigma(f \to \pi^+\pi^-)$(mb)	0.10 ± 0.02	0.17 ± 0.04	0.22 ± 0.04	0.005 ± 0.02	0.01 ± 0.01	0.51 ± 0.07
$<f \to \pi^+\pi^->$	0.018 ± 0.004	0.019 ± 0.004	0.045 ± 0.008	0.003 ± 0.01	0.06 ± 0.06	0.024 ± 0.004
$<f \to \pi^+\pi^->/<\pi^+>$	0.031 ± 0.007	0.014 ± 0.003	0.019 ± 0.003	0.001 ± 0.004	0.01 ± 0.01	0.015 ± 0.002
$<f \to \pi^+\pi^->/<\rho^o>$	0.38 ± 0.13	0.09 ± 0.02	0.14 ± 0.03	0.006 ± 0.02	0.1 ± 0.1	0.11 ± 0.02

TABLE 5

ρ^o IN EXCLUSIVE CHANNELS				
Prongs	Final state	Cross section (mb)	$\sigma(\rho^o)$ (mb)	$<\rho^o>$
2	$\pi^-\pi^+n$	0.68	0.055 ± 0.015	0.08
	$\pi^-\pi^+Z^o$	2.56	0.20 ± 0.04	0.08
4	$2\pi^-\pi^+p$	1.18	0.49 ± 0.07	0.42
	$2\pi^-\pi^+p\pi^o$	1.06	0.28 ± 0.03	0.26
	$2\pi^-\pi^+pZ^o$	3.16	0.38 ± 0.04	0.12
	$2\pi^-2\pi^+n$	0.60	0.39 ± 0.04	0.65
	$2\pi^-2\pi^+Z^o$	2.90	0.66 ± 0.09	0.23
6	$3\pi^-2\pi^+p$	0.28	0.17 ± 0.03	0.61
	$3\pi^-2\pi^+p\pi^o$	0.79	0.34 ± 0.04	0.43
	$3\pi^-2\pi^+pZ^o$	2.08	0.53 ± 0.08	0.25
	$3\pi^-3\pi^+n$	0.28	0.19 ± 0.03	0.68
	$3\pi^-3\pi^+Z^o$	1.42	0.53 ± 0.06	0.37
8	$4\pi^-3\pi^+p$	0.077	0.05 ± 0.01	0.65
	$4\pi^-3\pi^+p\pi^o$ $4\pi^-3\pi^+pZ^o$	0.81	0.35 ± 0.04	0.43
	$4\pi^-4\pi^+n$ $4\pi^-4\pi^+Z^o$	0.48	0.20 ± 0.03	0.42
10	$5\pi^-5\pi^+p\pi^o$ $5\pi^-4\pi^+pZ^o$	0.12	0.13 ± 0.05	1.09
ALL		18.48	4.9 ± 0.50	

TABLE 6

$\langle p_T^2 \rangle$ AND $\langle p_T \rangle$ FOR ρ^o, π^+ AND π^- PRODUCED IN $\pi^\pm p$ INTERACTIONS AT 16 GeV/c				
Particle	$\langle p_T^2 \rangle$ (GeV/c)^2		$\langle p_T \rangle$ (GeV/c)	
	$\pi^- p$	$\pi^+ p$	$\pi^- p$	$\pi^+ p$
ρ^o	0.29 ± 0.01	0.27 ± 0.01	0.45 ± 0.01	0.46 ± 0.01
π^+	0.154 ± 0.002	0.172 ± 0.002	0.329 ± 0.004	0.349 ± 0.004
π^-	0.164 ± 0.002	0.136 ± 0.002	0.343 ± 0.004	0.313 ± 0.004

FIGURE CAPTIONS

Fig. 1 The invariant mass spectrum of the $(\pi^+\pi^-)$ dipion system in the inclusive reaction $\pi^- p \to (\pi^+\pi^-)$ + anything at 16 GeV/c.

Fig. 2 The $(\pi^+\pi^-)$ invariant mass spectrum for different charged multiplicities.

Fig. 3 The inclusive invariant mass spectrum $d\sigma/dM(\pi^+\pi^-)$ multiplied by a factor exp(2.3M).

Fig. 4 The cross sections for (a) ρ^o, (b) $f \to \pi^+\pi^-$ and (c) f, as functions of charged multiplicity in $\pi^- p$ and $\pi^+ p$ interactions at 16 GeV/c. The cross sections for f are deduced from the measured semi-inclusive cross sections for the partial mode $f \to \pi^+\pi^-$ and the known branching ratios of the f - decay.

Fig. 5 The ratios $R(\pi^+ p) = \langle\rho^o\rangle/\langle\pi^-\rangle$ for $\pi^+ p$ interactions at 16 GeV/c and $\langle\rho^o\rangle/\langle\pi^+\rangle$ and $R(\pi^- p) = \langle\rho^o\rangle/(\langle\pi^-\rangle - 1)$ for $\pi^- p$ interactions at 16 GeV/c as functions of the charged multiplicity.

Fig. 6 $\sigma(\rho^o)$ as a function of s, the c.m. energy squared, for $\pi^- p$, $\pi^+ p$ and pp interactions. The solid line is a fit to the $\pi^\pm p$ data, of the form given by eq. (2). The dashed line is a similar fit to the pp data with the slope constrained to that of the solid line.

Fig. 7 (a) $\langle\rho^o\rangle$ as a function of s for $\pi^- p$, $\pi^+ p$ and pp interactions. The solid line is a simple logarithmic fit (see text) to the $\pi^\pm p$ data. The dashed line is a similar fit to the pp data with the slope constrained to that of the solid line.

(b) The energy dependence of the inclusive ratios $\langle\rho^o\rangle/\langle\pi^-\rangle$ for $\pi^+ p$, pp and $\langle\rho^o\rangle/(\langle\pi^-\rangle - 1)$ for $\pi^- p$ interactions. The solid curve is a prediction based on the solid line in fig. 7(a) and eq. (6).

Likewise, the dotted line is a prediction based on the dotted line in fig. 7(a) and a fit to the experimental data on the energy dependence of $<\pi^->$ in pp collisions.

Fig. 8 The inclusive distribution of the transverse momentum squared for the ρ^o and π^+ for π^-p interactions at 16 GeV/c. Also shown are a few representative points for the π^-. The dotted curves represent simple exponential fits described in the text.

Fig. 9 The variation with transverse momentum squared of the ratio of the production cross section of ρ^o to that of the π^+. The dashed line corresponds to a value of 0.54, which is the weighted mean of the ratio for $p_T^2 > 0.8$ $(GeV/c)^2$.

Fig. 10 (a) The differential cross section for ρ^o per unit of x and of p_T for different intervals of p_T.

(b) The differential cross section for ρ^o per unit of x, integrated over all p_T.

Fig. 11 (a) The invariant differential cross section for ρ^o as a function of x for the same intervals in p_T as in fig. 10.

(b) The ρ^o invariant cross section integrated over p_T^2 as a function of x.

Fig. 12 Comparison of x distributions for ρ^o invariant cross section in π^-p and π^+p interactions at 16 GeV/c. Also shown is the x distribution for the exclusive channel $\pi^-p \to \rho^o n$.

Fig. 13 Comparison of the invariant x distribution of ρ^o, π^+ and π^- in π^-p interactions and of $K^{*o}(890)$ in K^-p interactions at 16 GeV/c [14].

Fig. 14 Invariant x distribution for inclusive and semi-inclusive ρ^o production in π^-p interactions at 16 GeV/c. The curves drawn are merely to guide the eye.

Fig. 15 Distribution of the ρ^o rapidity in the beam frame, $y_b(\rho^o) = y_{beam} - y(\rho^o)$, in $\pi^- p$ interactions at 16 GeV/c and comparison with similar data at 147 [8] and 205 [9] GeV/c. The arrow corresponds to the rapidity of the ρ^o emitted at 90^o in the c.m. system for 16 GeV/c $\pi^- p$ interactions and the maximum value of $y_b(\rho^o)$ is 1.7, for the central value of the ρ^o mass.

Fig. 16 Comparison of the c.m. rapidity distribution of ρ^o in 16 GeV/c $\pi^- p$ interactions with the same in 16 GeV/c $\pi^+ p$ [5] and 24 GeV/c pp interactions [3].

Fig. 17 The x distribution of the difference between the invariant cross section for $\pi^- p \to \rho^o X^o$ and the invariant cross section for $K^- p \to K^{*o}(890) X^o$ [14], both at 16 GeV/c.

Fig. 1

NUMBER OF COMBINATIONS (10^4/40 MeV)
2
1
0
$(\pi^+\pi^-)$ MASS SPECTRUM IN $\pi^- p \to \pi^+\pi^-$ +ANYTHING
AT 16 GeV/c
$\rho^0(770)$
f (1270)
0.5
1.0
1.5
2.0
M $(\pi^+\pi^-)$, GeV
$d\sigma/dM$, mb/40 MeV
4
2
0

Fig. 2

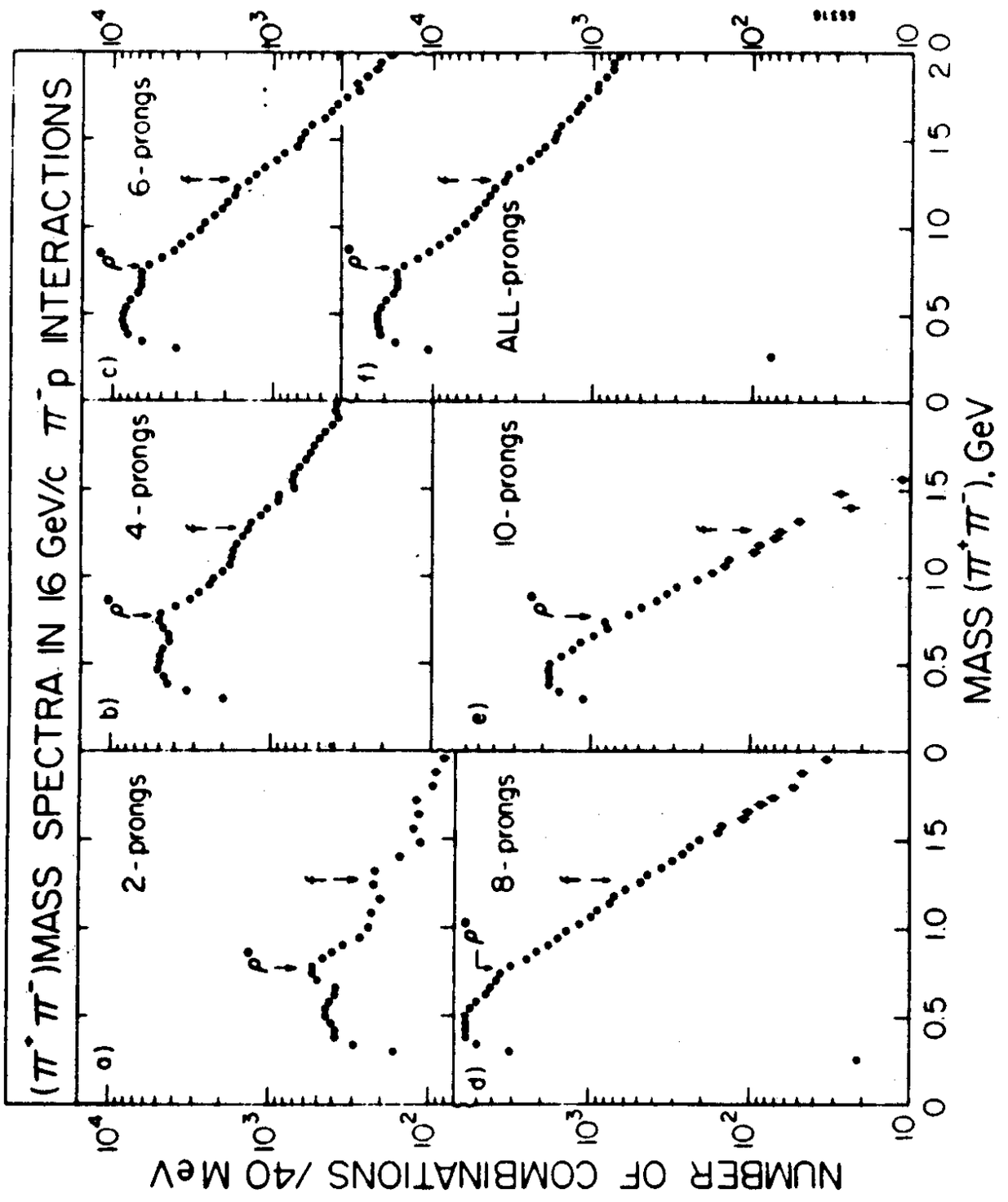
$(\pi^+\pi^-)$MASS SPECTRA IN 16 GeV/c π^-p INTERACTIONS
a) 2-prongs
b) 4-prongs
c) 6-prongs
d) 8-prongs
e) 10-prongs
f) ALL-prongs
ρ
f
NUMBER OF COMBINATIONS /40 MeV
MASS $(\pi^+\pi^-)$, GeV

Fig. 3

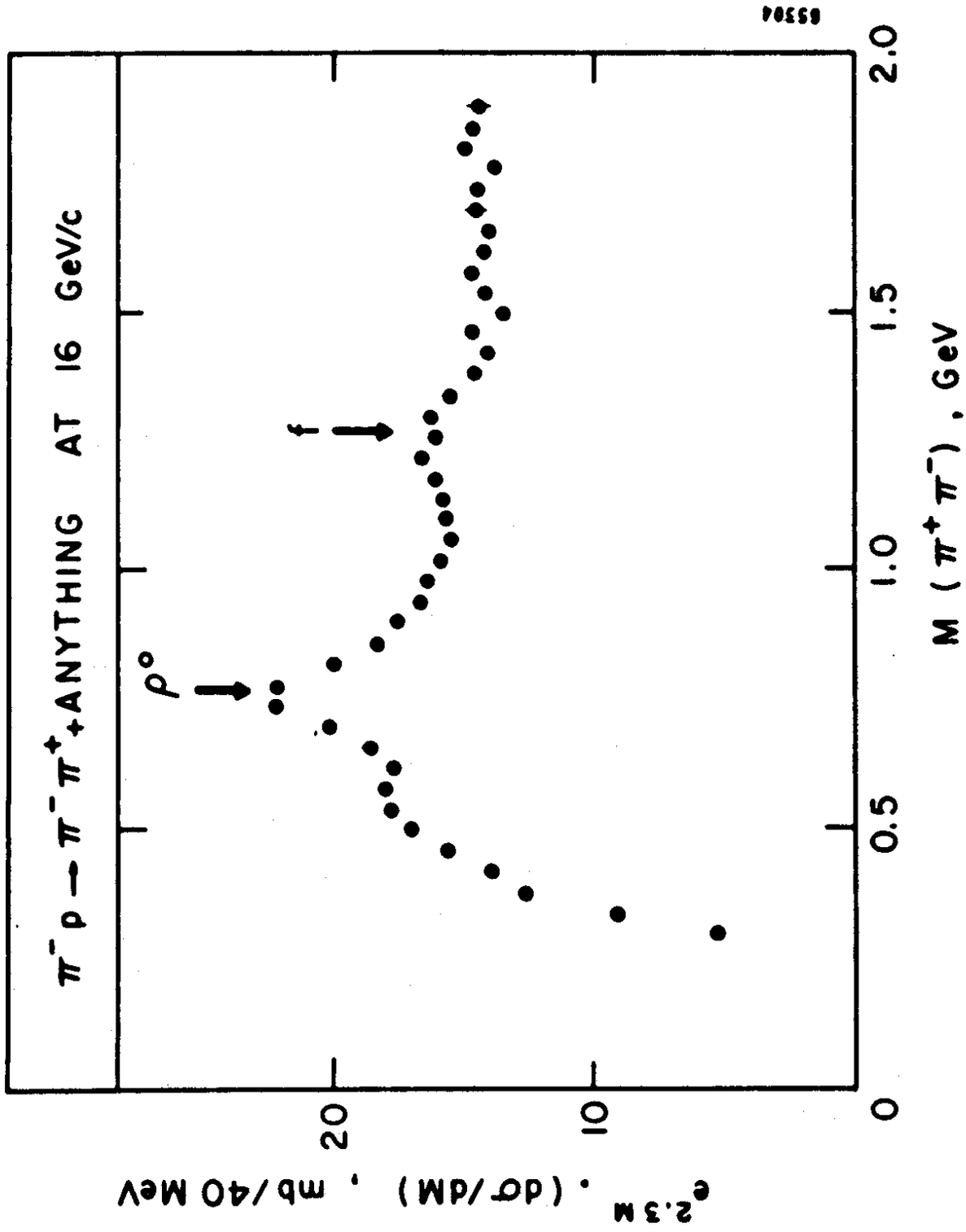
65304
$\pi^- p \to \pi^- \pi^+ +$ANYTHING AT 16 GeV/c
ρ^0
f
0
0.5
1.0
1.5
2.0
M ($\pi^+\pi^-$), GeV
20
10
$e^{2.3M}$. (dσ/dM) , mb/40 MeV

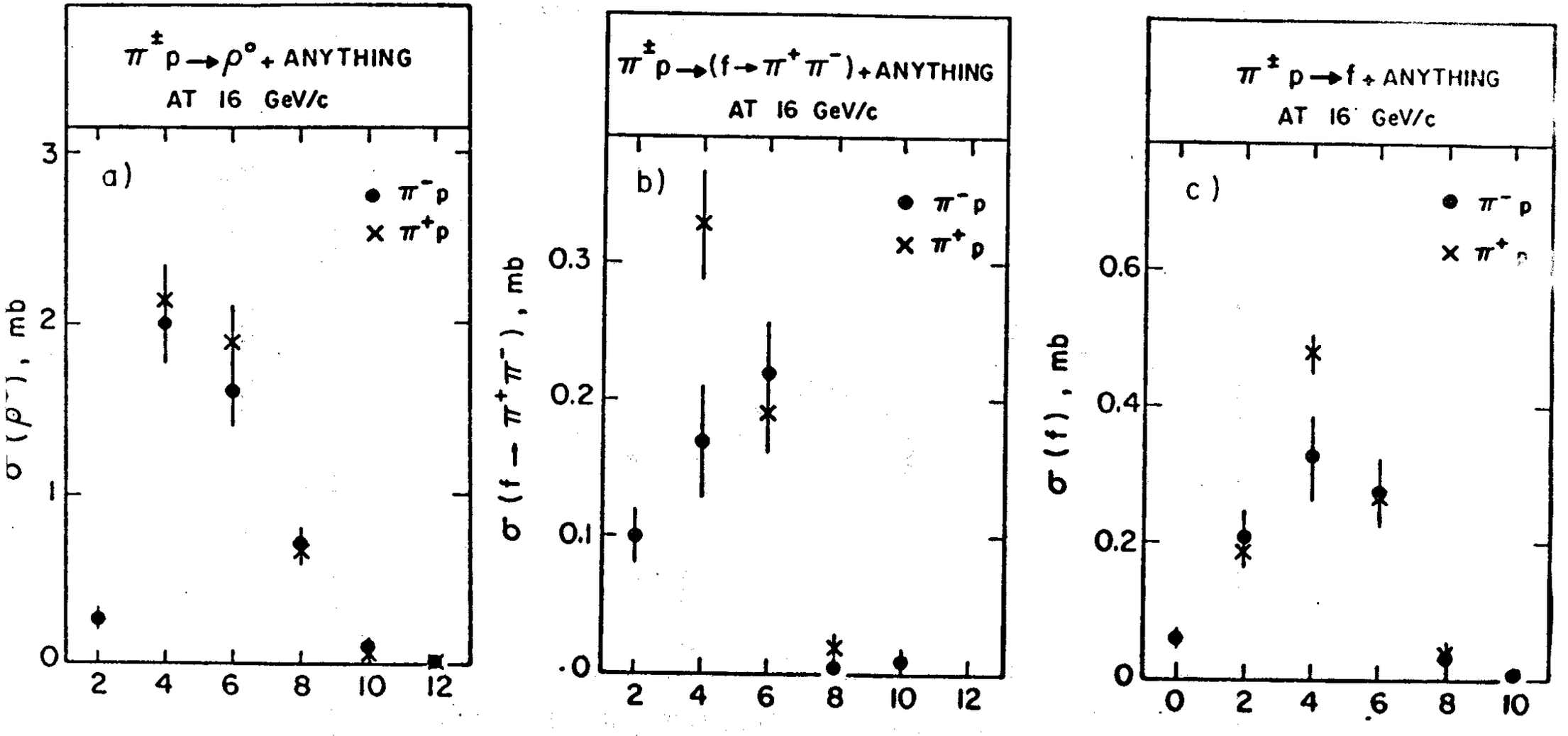
$\pi^{\pm} p \rightarrow \rho^{0}$ + ANYTHING
AT 16 GeV/c
a)
$\pi^- p$
$\pi^+ p$
$\sigma(\rho^0)$, mb
$\pi^{\pm} p \rightarrow (f \rightarrow \pi^+ \pi^-)$ + ANYTHING
AT 16 GeV/c
b)
$\sigma(f \rightarrow \pi^+ \pi^-)$, mb
$\pi^{\pm} p \rightarrow f$ + ANYTHING
AT 16 GeV/c
c)
$\sigma(f)$, mb
CHARGED MULTIPLICITY

Fig. 4

Fig. 5

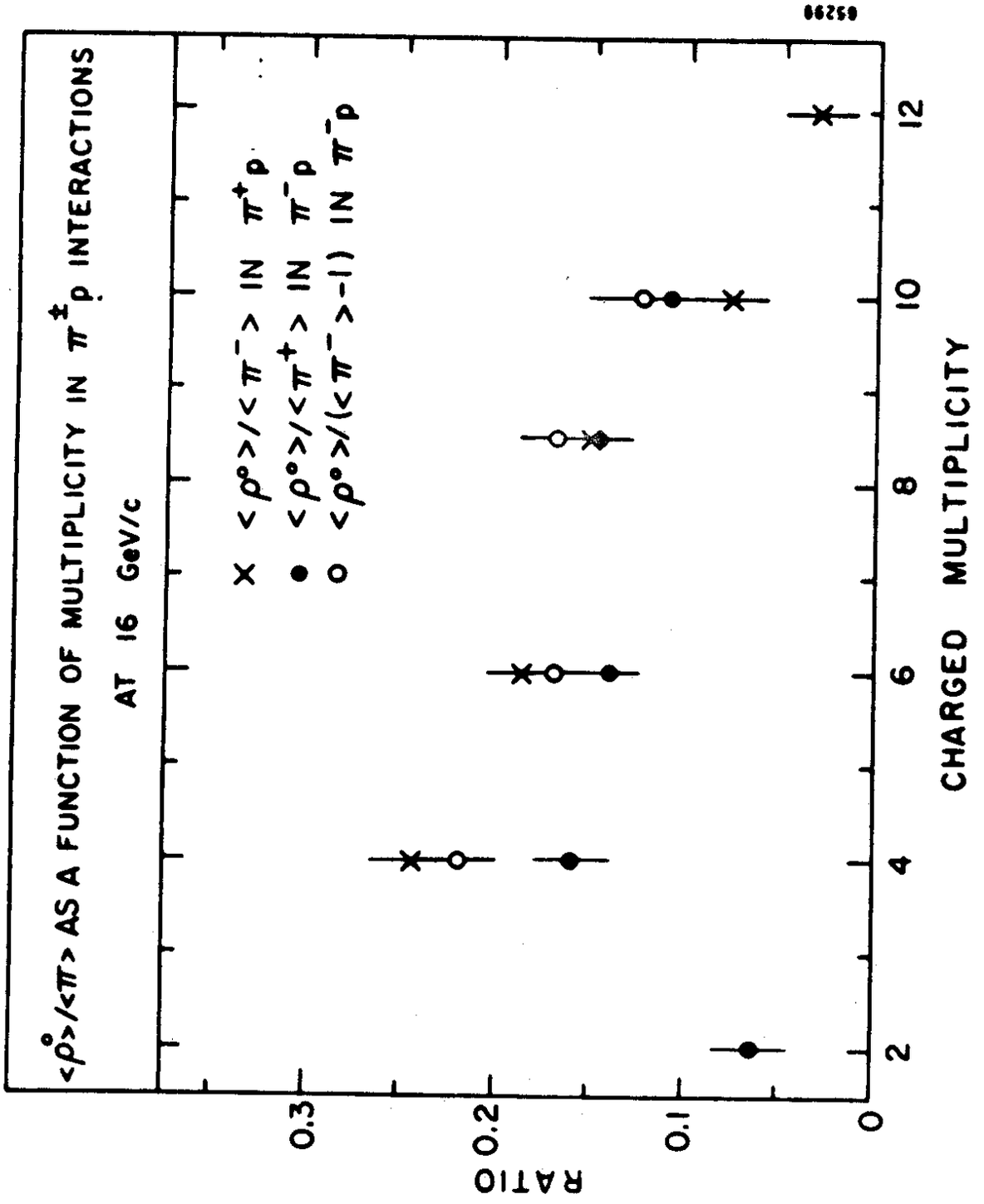
65259
$\langle\rho^0\rangle/\langle\pi\rangle$ AS A FUNCTION OF MULTIPLICITY IN $\pi^\pm p$ INTERACTIONS
AT 16 GeV/c
X $\langle\rho^0\rangle/\langle\pi^-\rangle$ IN $\pi^+ p$
● $\langle\rho^0\rangle/\langle\pi^+\rangle$ IN $\pi^- p$
○ $\langle\rho^0\rangle/(\langle\pi^-\rangle-1)$ IN $\pi^- p$
RATIO
0.3
0.2
0.1
0
2
4
6
8
10
12
CHARGED MULTIPLICITY

Fig. 6

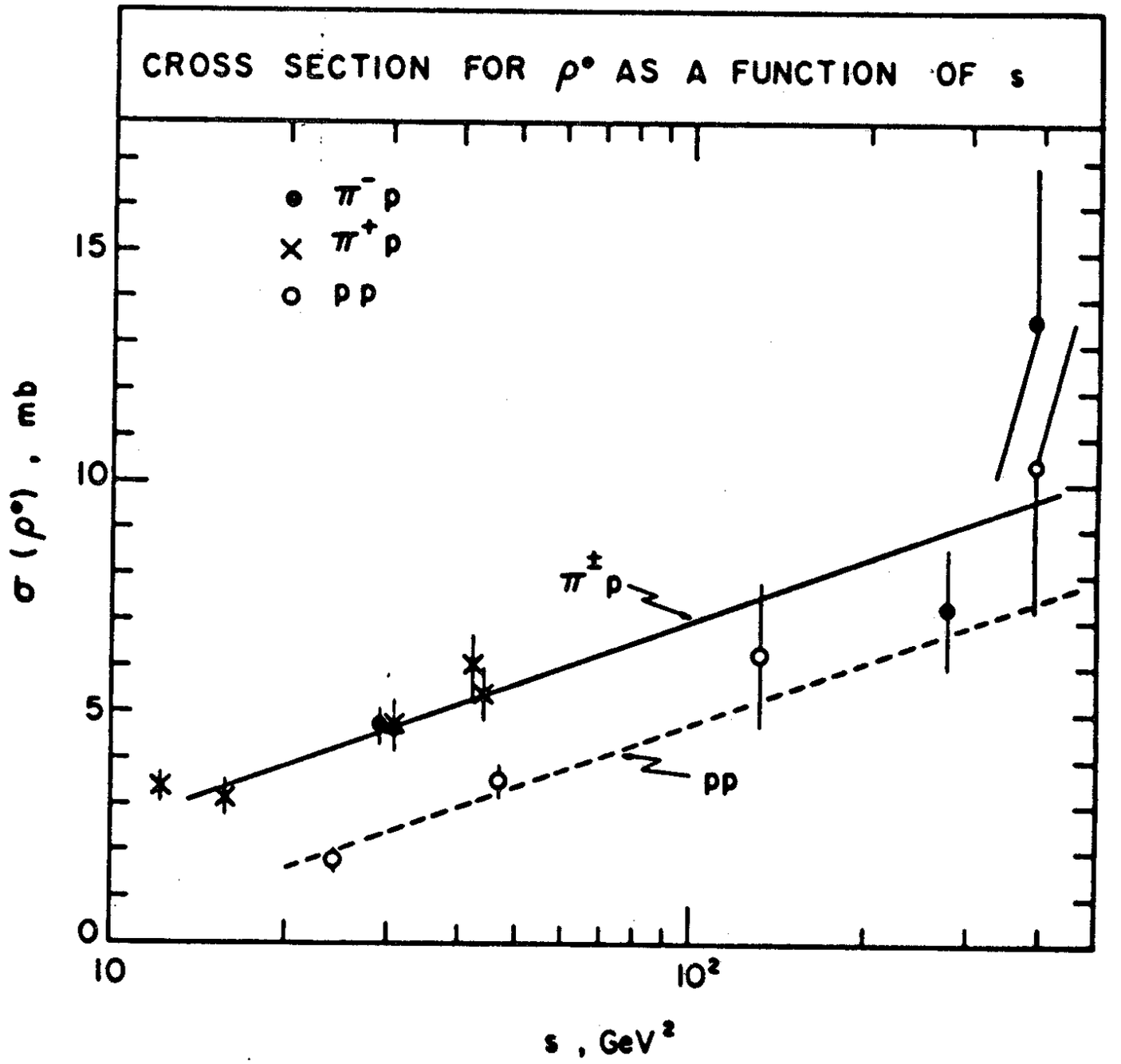
CROSS SECTION FOR ρ° AS A FUNCTION OF s
π⁻p
π⁺p
pp
π±p
pp
σ (ρ°) , mb
s , GeV²
0
5
10
15
10
10²

Fig. 7

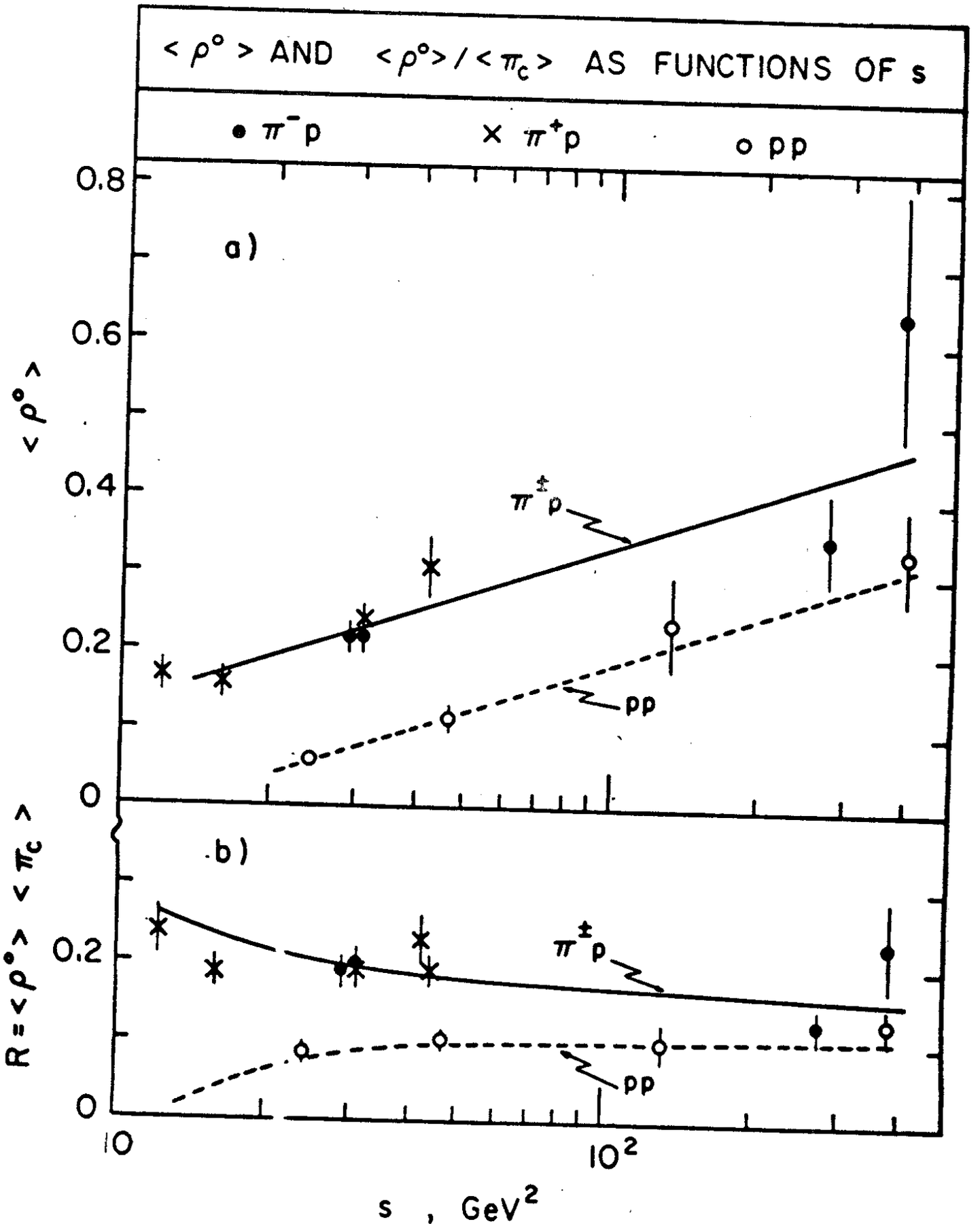
< ρ° > AND < ρ° > / < π_c > AS FUNCTIONS OF s
• π⁻p
× π⁺p
o pp
a)
b)
< ρ° >
R = < ρ° > < π_c >
π±p
pp
0.8
0.6
0.4
0.2
0
10
10²
s , GeV²

Fig. 8

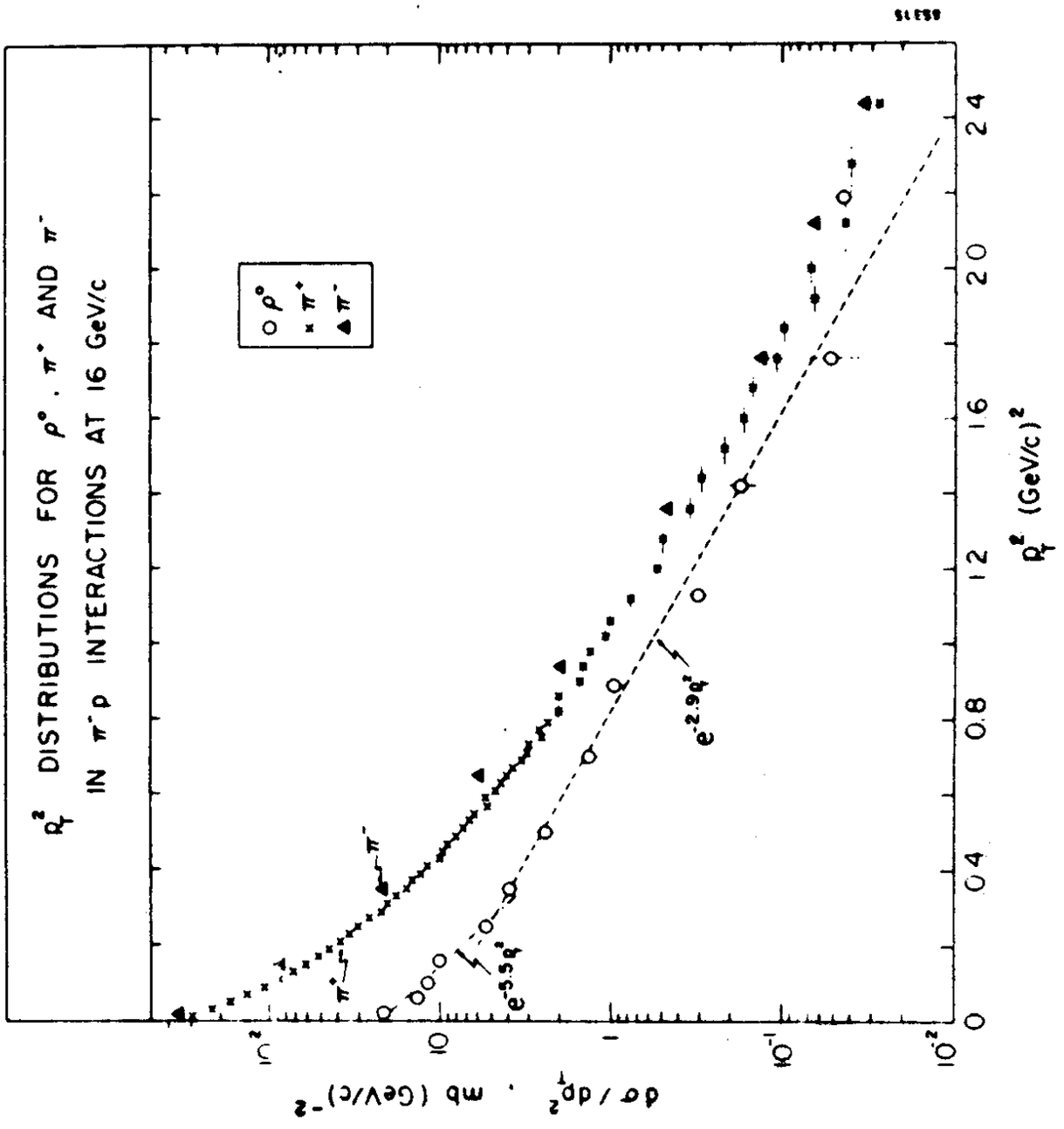
p_T^2 DISTRIBUTIONS FOR ρ^0, π^+ AND π^-
IN $\pi^- p$ INTERACTIONS AT 16 GeV/c
ρ^0
π^+
π^-
$e^{-5.5 p_T^2}$
$e^{-2.9 p_T^2}$
$d\sigma / dp_T^2$, mb (GeV/c)$^{-2}$
p_T^2 (GeV/c)^2
0
0.4
0.8
1.2
1.6
2.0
2.4
10^{-2}
10^{-1}
1
10^1
10^2

Fig. 9

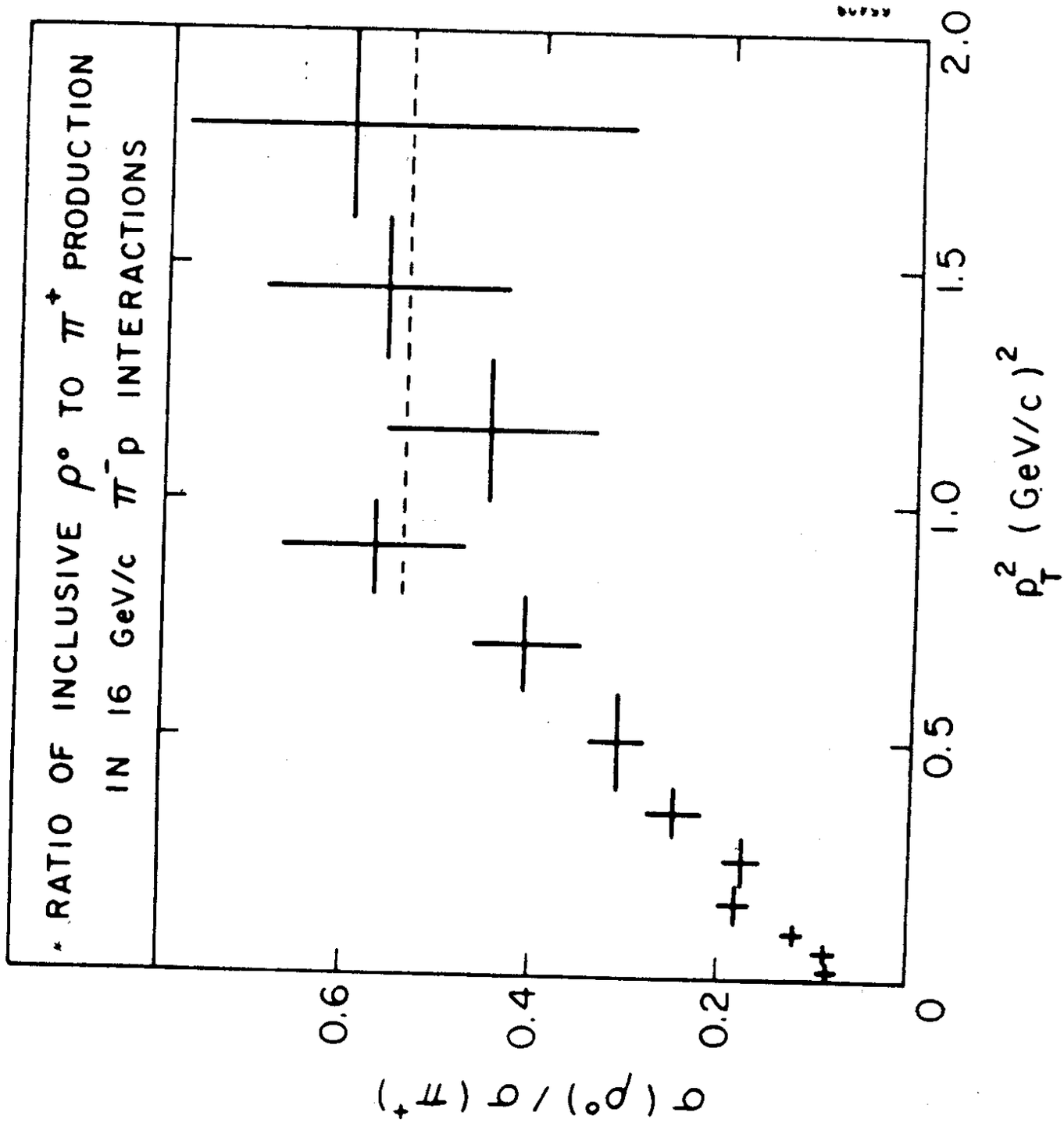
* RATIO OF INCLUSIVE ρ° TO π⁺ PRODUCTION
IN 16 GeV/c π⁻p INTERACTIONS
σ (ρ°) / σ (π⁺)
0.6
0.4
0.2
0
0.5
1.0
1.5
2.0
p_T^2 (GeV/c)^2

Fig. 10

CROSS SECTIONS IN x AND p_T FOR ρ^0

IN $\pi^- p \rightarrow \pi^+ \pi^- +$ ANYTHING AT 16 GeV/c

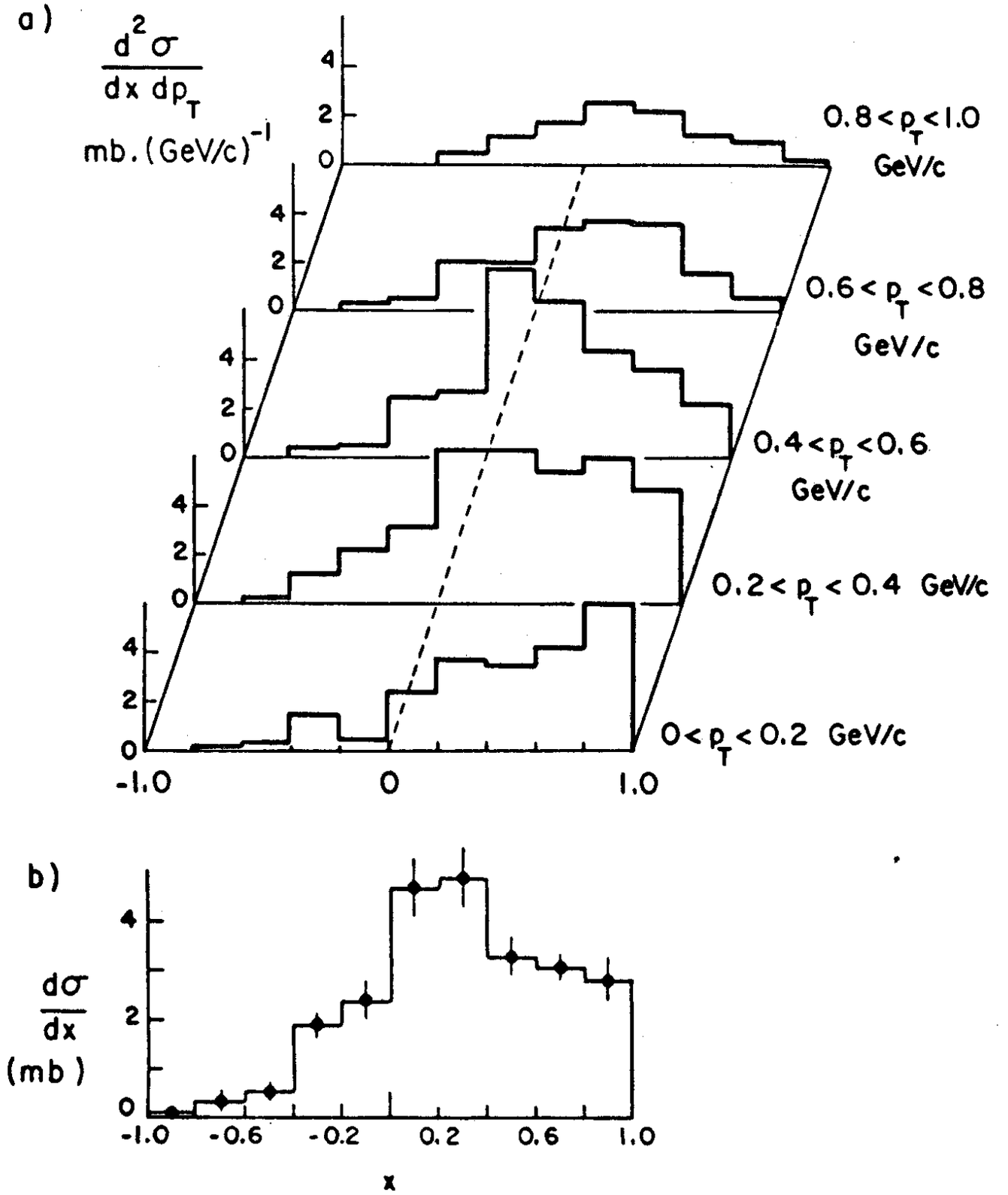

Fig. 11

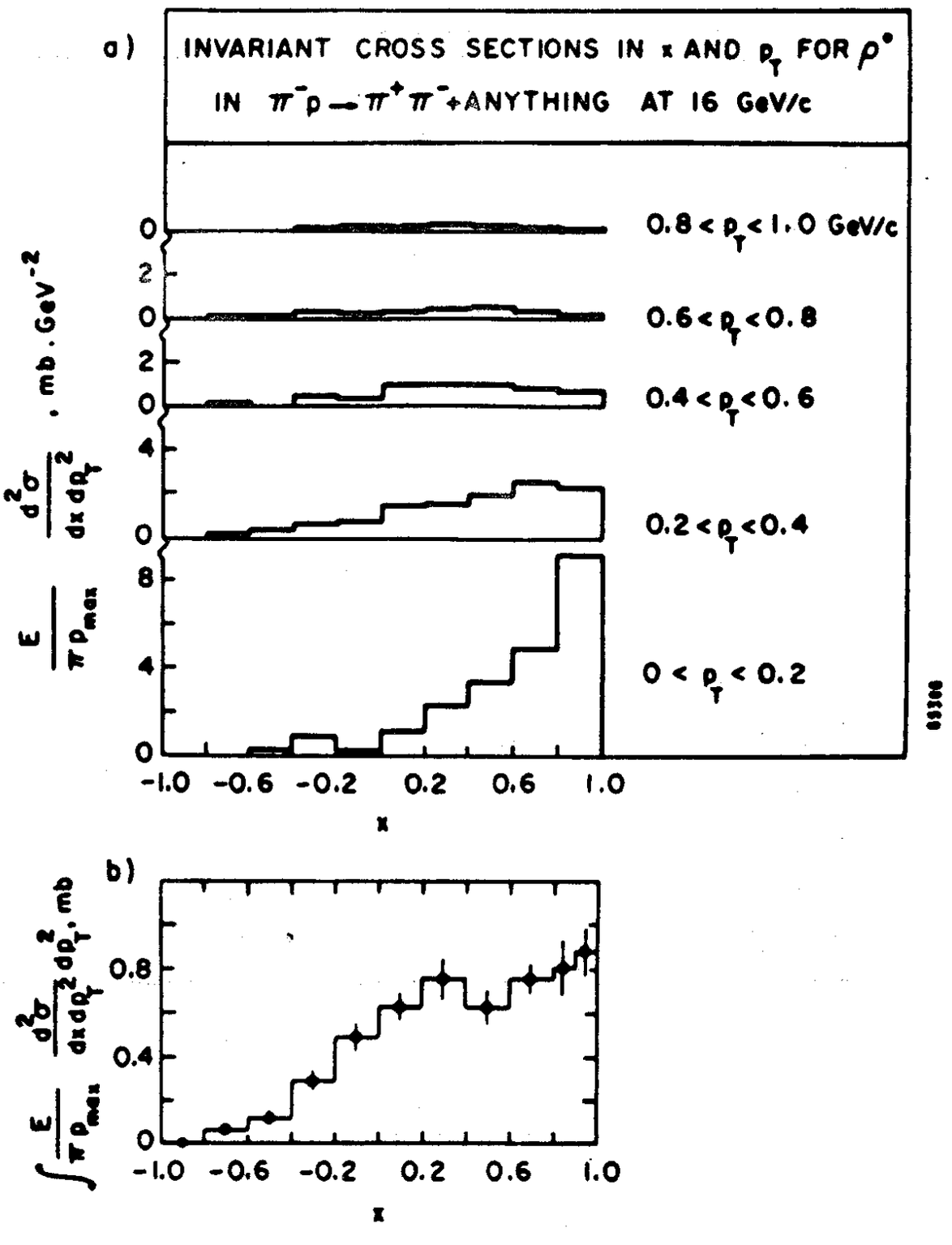
a)
INVARIANT CROSS SECTIONS IN x AND p_T FOR ρ^0
IN $\pi^- p \to \pi^+ \pi^-$ + ANYTHING AT 16 GeV/c
$\frac{E}{\pi p_{max}} \frac{d^2\sigma}{dx\, dp_T^2}$, mb. GeV^{-2}
$0.8 < p_T < 1.0$ GeV/c
$0.6 < p_T < 0.8$
$0.4 < p_T < 0.6$
$0.2 < p_T < 0.4$
$0 < p_T < 0.2$
0
2
0
2
0
4
0
8
4
0
-1.0 -0.6 -0.2 0.2 0.6 1.0
x
b)
$\int \frac{E}{\pi p_{max}} \frac{d^2\sigma}{dx\, dp_T^2} dp_T^2$, mb
0.8
0.4
0
-1.0 -0.6 -0.2 0.2 0.6 1.0
x

Fig. 12

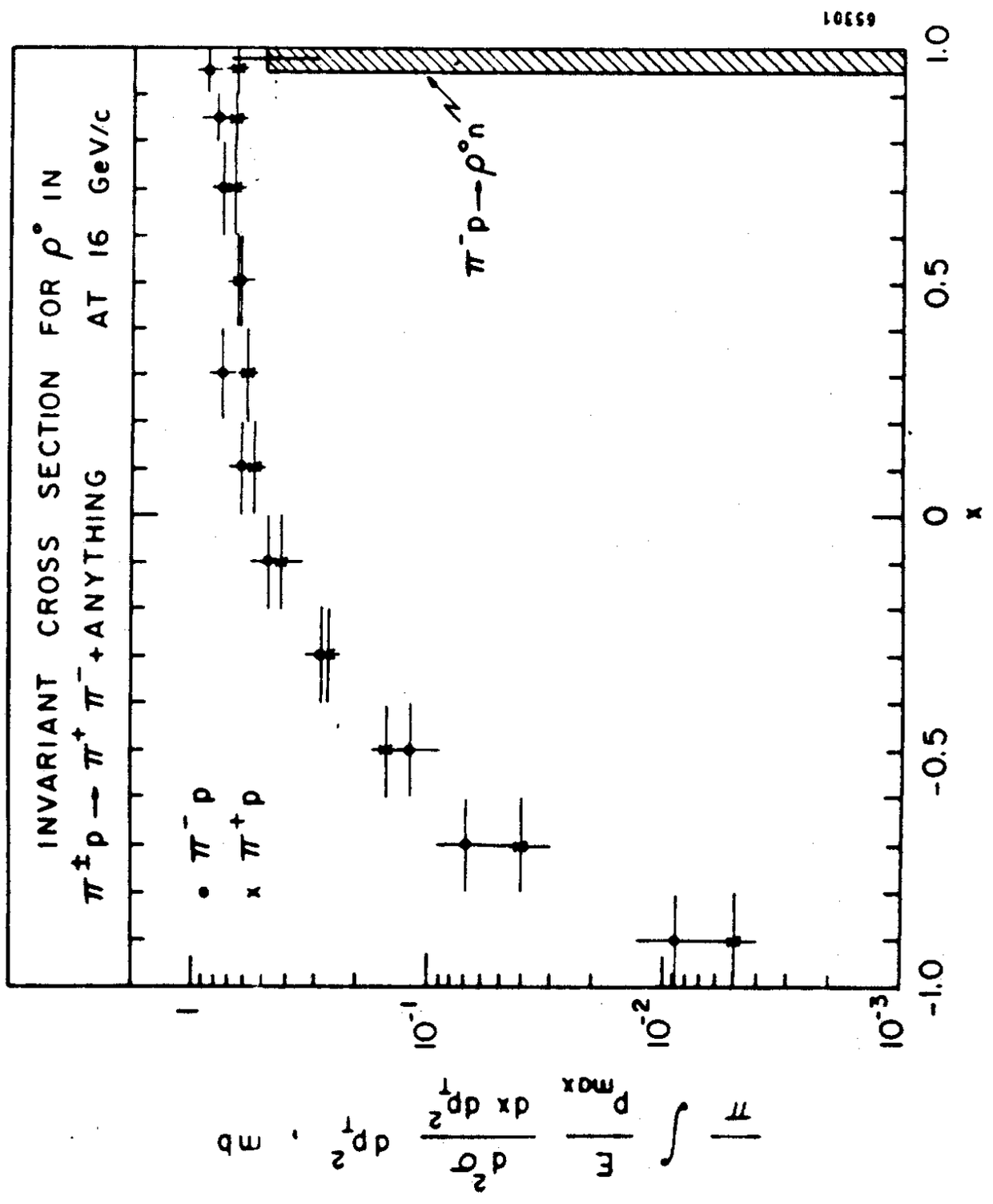
65301
INVARIANT CROSS SECTION FOR ρ° IN
π±p → π⁺π⁻+ANYTHING AT 16 GeV/c
• π⁻p
× π⁺p
π⁻p→ρ°n
1
10⁻¹
10⁻²
10⁻³
1.0
0.5
0
-0.5
-1.0
x
$\frac{\pi}{p_{max}} \int \frac{E}{dx\, dp_T^2} \frac{d^2\sigma}{dp_T^2} \cdot mb$

Fig. 13

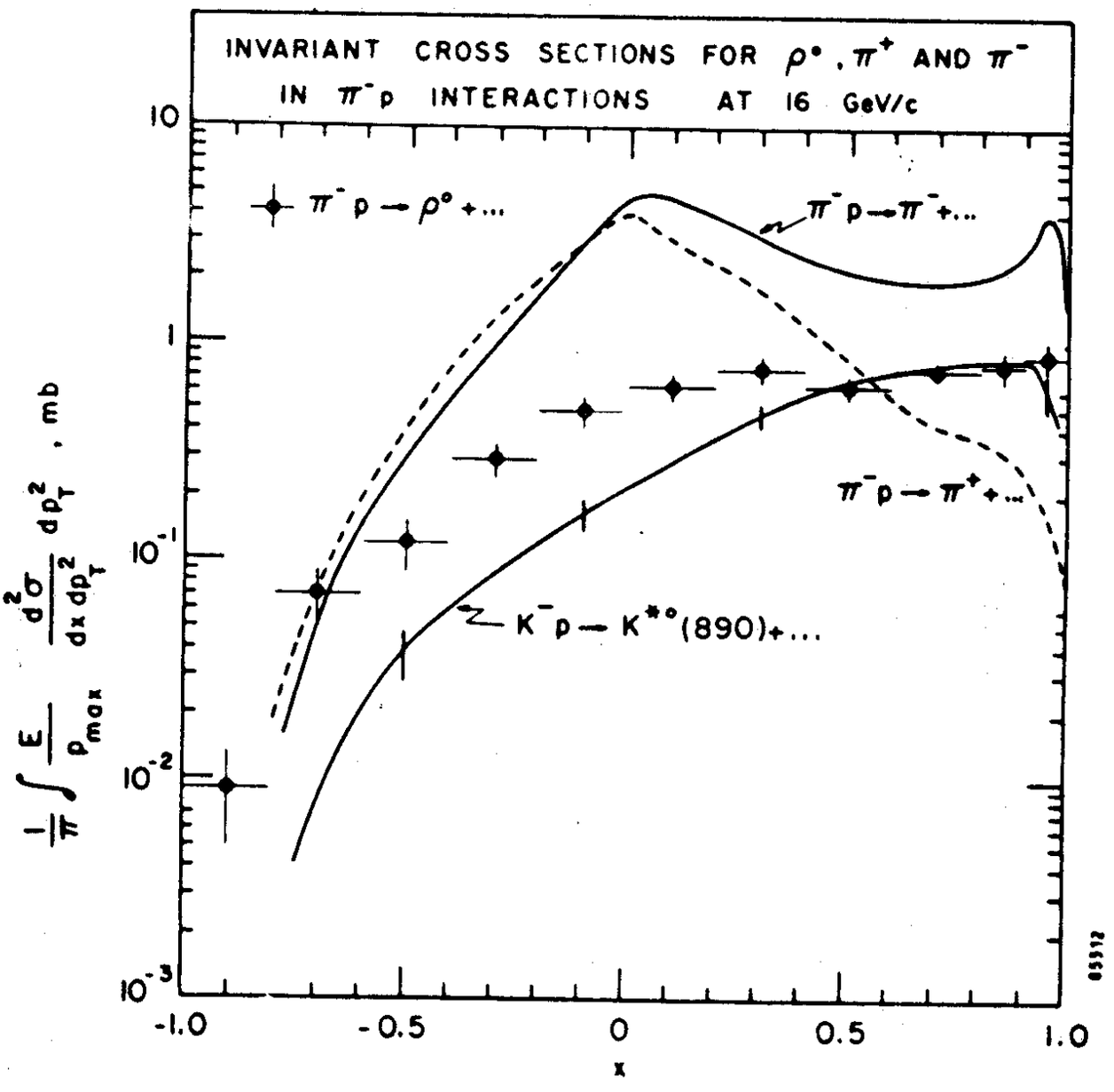
INVARIANT CROSS SECTIONS FOR ρ°, π⁺ AND π⁻
IN π⁻p INTERACTIONS AT 16 GeV/c
π⁻p → ρ°+...
π⁻p → π⁻+...
π⁻p → π⁺+...
K⁻p → K*°(890)+...
10
1
10⁻¹
10⁻²
10⁻³
-1.0
-0.5
0
0.5
1.0
x
1/π ∫ E/p_max d²σ/dx dp_T² dp_T², mb
85512

Fig. 14

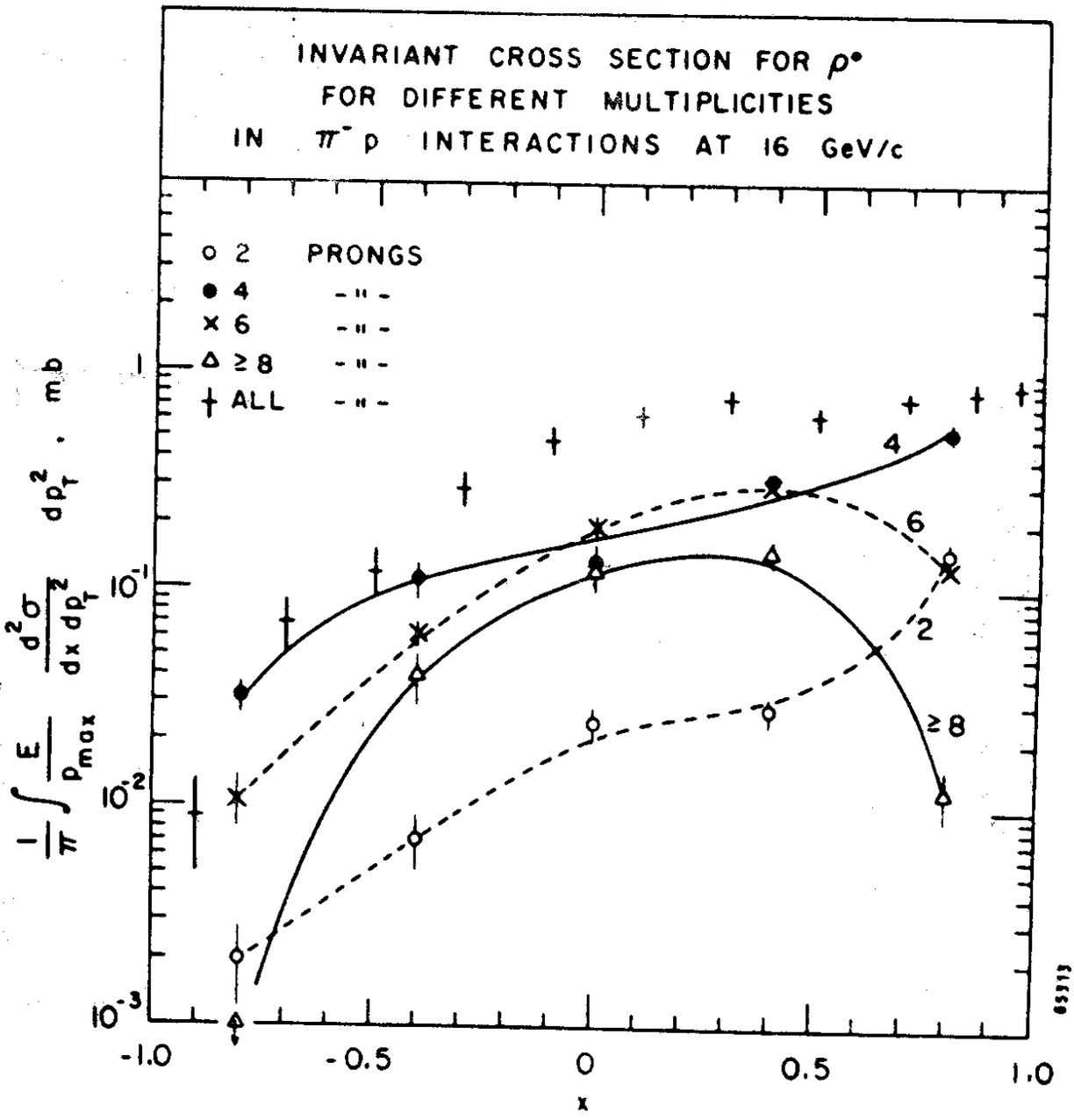
INVARIANT CROSS SECTION FOR ρ°
FOR DIFFERENT MULTIPLICITIES
IN π⁻p INTERACTIONS AT 16 GeV/c
○ 2 PRONGS
● 4 -"-
× 6 -"-
△ ≥8 -"-
† ALL -"-
$\frac{1}{\pi}\int \frac{E}{p_{max}} \frac{d^2\sigma}{dx\,dp_T^2}\,dp_T^2$, mb
1
10^{-1}
10^{-2}
10^{-3}
-1.0
-0.5
0
0.5
1.0
x
4
6
2
≥8
65113

Fig. 15

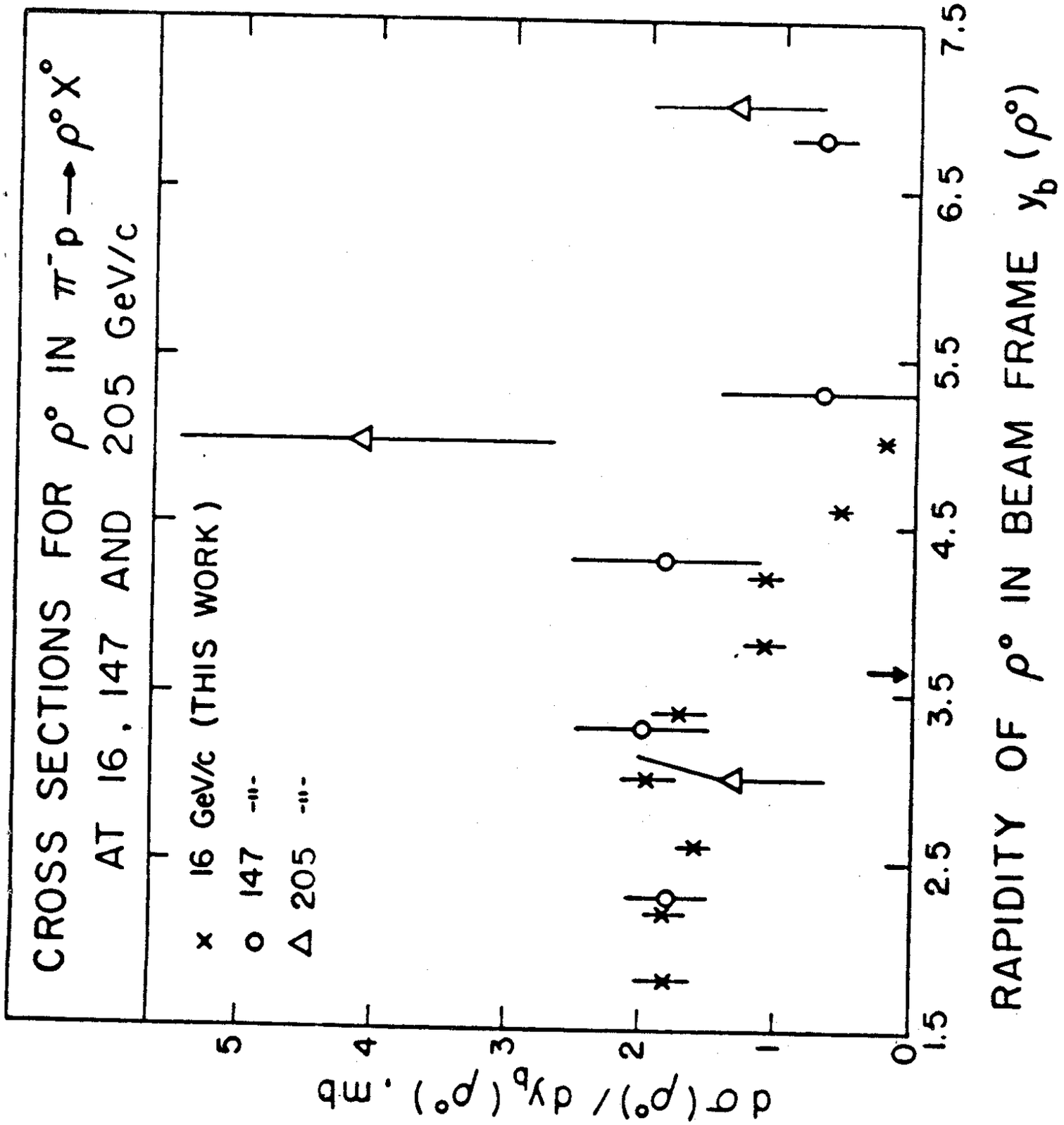
CROSS SECTIONS FOR ρ° IN π⁻p → ρ°X°
AT 16, 147 AND 205 GeV/c
× 16 GeV/c (THIS WORK)
○ 147 -"-
△ 205 -"-
dσ(ρ°)/dy_b(ρ°) . mb
RAPIDITY OF ρ° IN BEAM FRAME y_b(ρ°)
0
1
2
3
4
5
1.5
2.5
3.5
4.5
5.5
6.5
7.5

Fig. 16

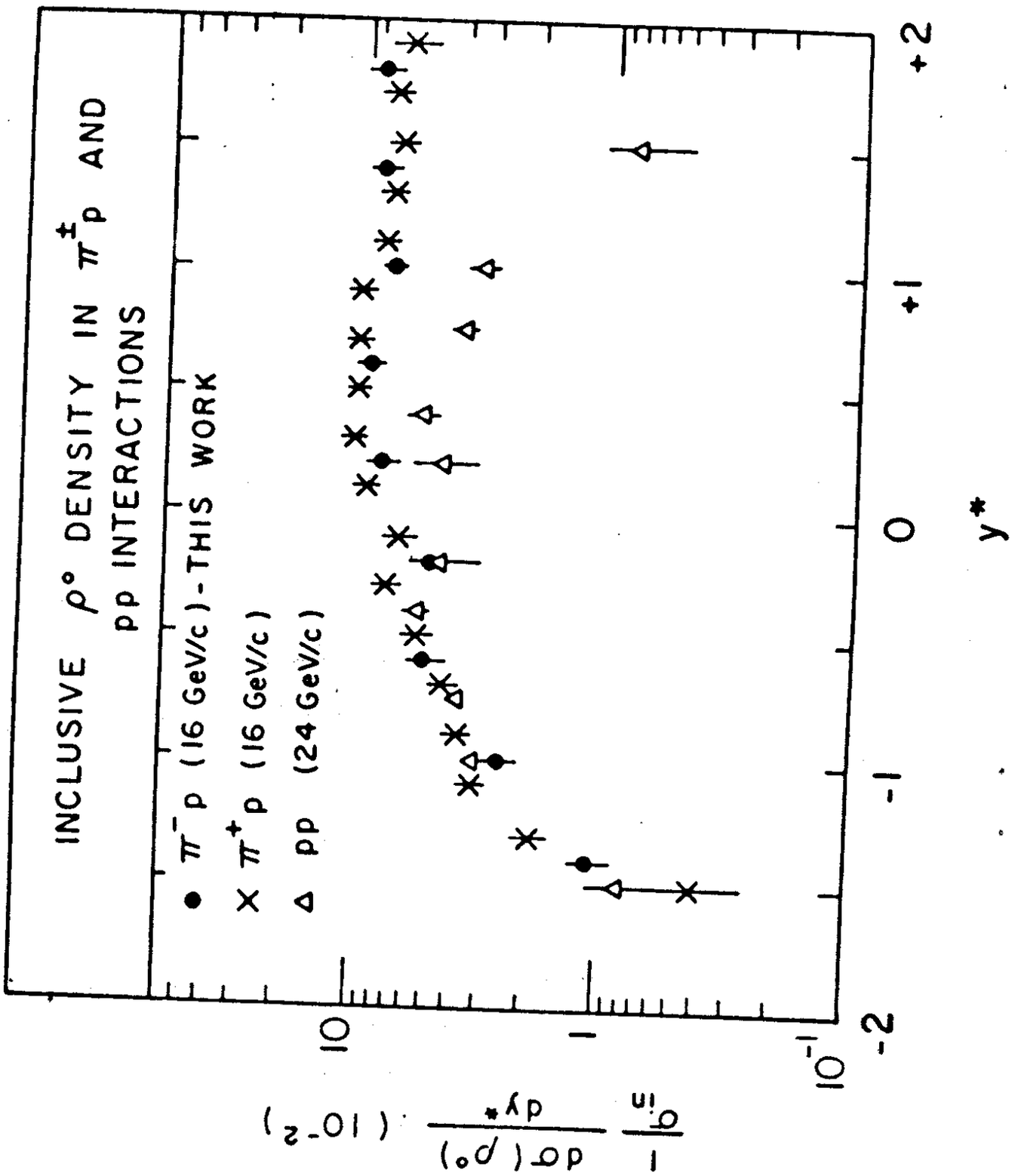
INCLUSIVE ρ° DENSITY IN π±p AND pp INTERACTIONS
• π⁻p (16 GeV/c) - THIS WORK
× π⁺p (16 GeV/c)
△ pp (24 GeV/c)
10
1
10⁻¹
-2
-1
0
+1
+2
y*
1/σin dσ(ρ°)/dy* (10⁻²)

Fig. 17

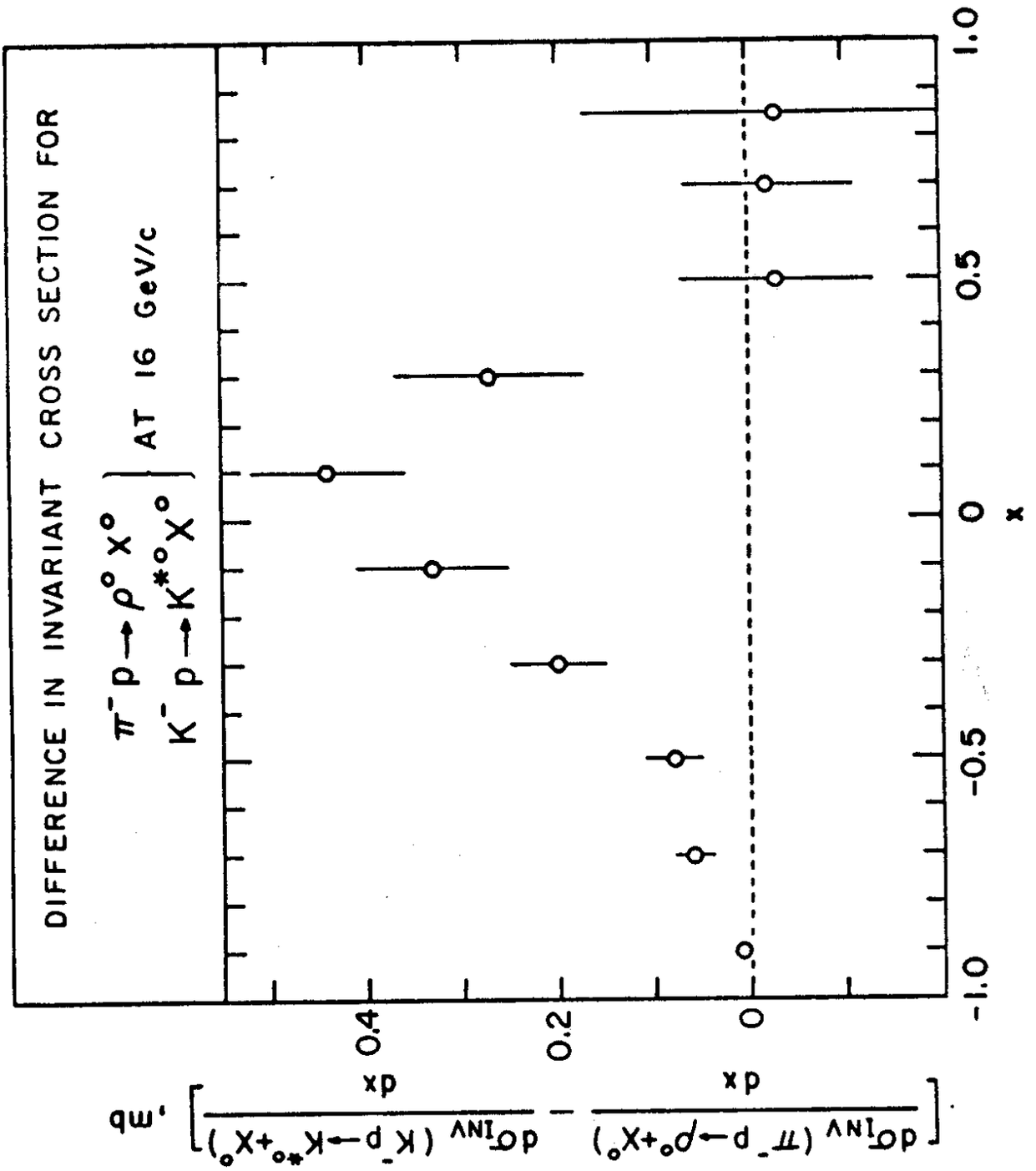
DIFFERENCE IN INVARIANT CROSS SECTION FOR
$\pi^- p \to \rho^0 X^0$
$K^- p \to K^{*0} X^0$
AT 16 GeV/c
1.0
0.5
0
-0.5
-1.0
x
0.4
0.2
0
$\frac{d\sigma_{INV}}{dx}$
$\frac{d\sigma_{INV}}{dx}$
$\left[\frac{d\sigma_{INV}(\pi^- p \to \rho^0 + X^0)}{dx} - \frac{d\sigma_{INV}(K^- p \to K^{*0} + X^0)}{dx}\right]$, mb